Waikato Regional Council Technical Report 2017/12

Remote sensing of Waikato lakes

www.waikatoregion.govt.nz
ISSN 2230-4355 (Print)
ISSN 2230-4363 (Online)

Waikato
REGIONAL COUNCIL
Te Kaunihera ā Rohe o Waikato

Prepared by:
Mathew Allan
The University of Waikato

For:
Waikato Regional Council
Private Bag 3038
Waikato Mail Centre
HAMILTON 3240

2016

Document #: 10188039

Peer reviewed by:
Deniz Özkundakci Date March 2017

Approved for release by:
Dominique Noiton
Date April 2017

Disclaimer

This technical report has been prepared for the use of Waikato Regional Council as a reference document and as such does not constitute Council's policy.

Council requests that if excerpts or inferences are drawn from this document for further use by individuals or organisations, due care should be taken to ensure that the appropriate context has been preserved, and is accurately reflected and referenced in any subsequent spoken or written communication.

While Waikato Regional Council has exercised all reasonable skill and care in controlling the contents of this report, Council accepts no liability in contract, tort or otherwise, for any loss, damage, injury or expense (whether direct, indirect or consequential) arising out of the provision of this information or its use by you or any other party.

Remote sensing of Waikato lakes

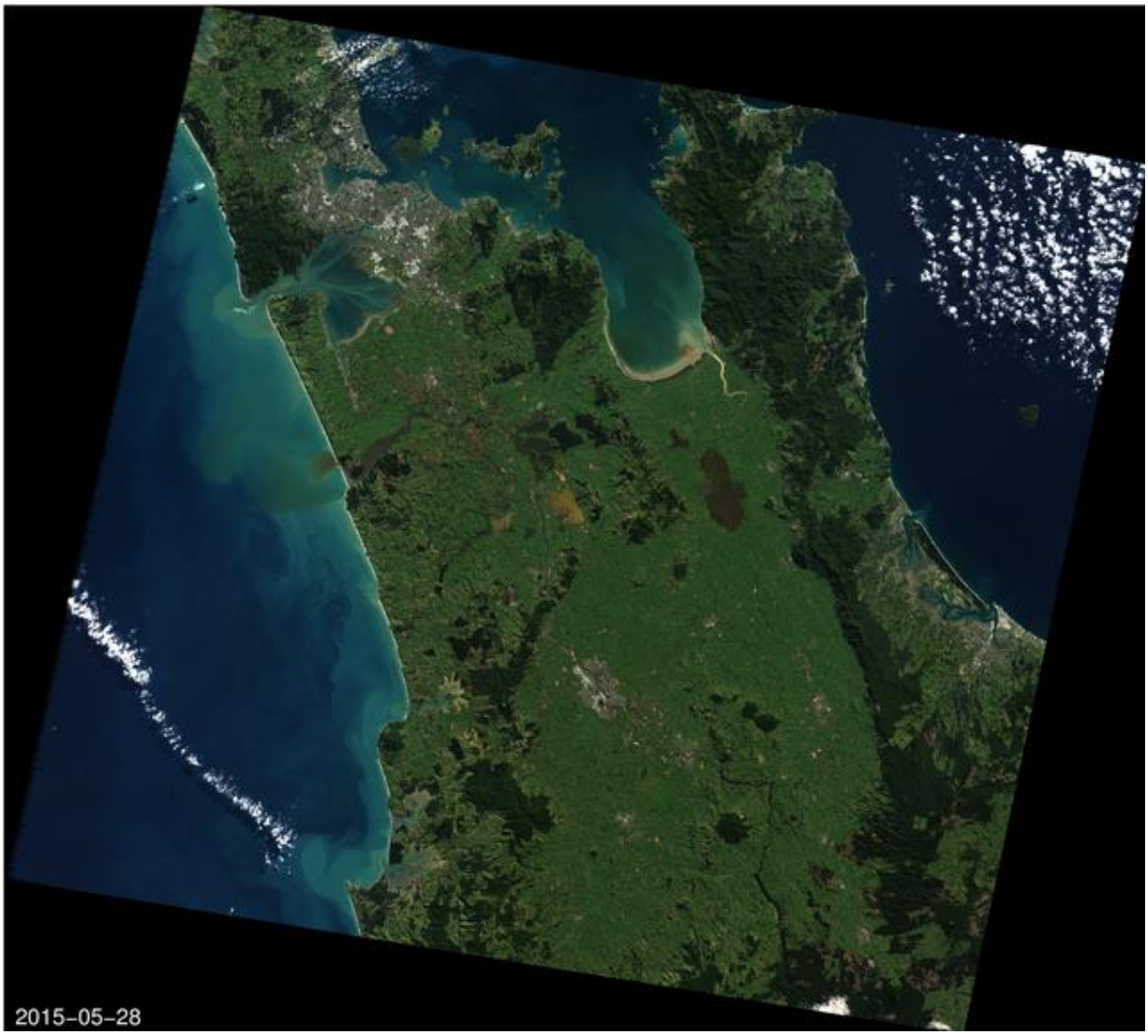

2016
ERI report 93

Prepared for Waikato Regional Council
By Mathew Allan

Environmental Research Institute
Te Pūtahi Rangahau Taiao
THE UNIVERSITY OF WAIKATO

THE UNIVERSITY OF WAIKATO
Te Whare Wānanga o Waikato

Contributing author

Mathew Allan, University of Waikato, Hamilton

Cover photo

Landsat seven image captured 28/5/2015

Reviewed by:

Uyen Nguyen

Research Fellow

Approved for release by:

John Tyrrell

Business Manager

Environmental Research Institute

The University of Waikato

Table of Contents

Table of Contents 7
List of figures 8
List of tables 9
Executive summary 10
Introduction 11
  Objectives 12
Methods 14
  Waikato lakes study site 14
  Remote sensing 16
    Satellite imagery, software and in situ data 16
    Linear spectral unmixing 18
    Watercolour 18
Results 20
  Total suspended solids (TSS) 20
  Chlorophyll a 27
  Chromaticity analysis 29
Discussion 31
Conclusions 32
References 33
Appendix 35

List of figures

Figure 1. Waikato study site map including lakes and estuaries 15
Figure 2. The empirical relationship between average subsurface remote sensing reflectance (r_{rs}) in Landsat B2B3 and total suspended solids (TSS, mg L^{-1}). 21
Figure 3. *In situ* TSS versus estimated TSS using the empirical relationship between average subsurface remote sensing reflectance (r_{rs}) in Landsat B2B3 and total suspended solids (TSS, mg L^{-1}). 21
Figure 4. *In situ* TSS versus estimated TSS using symbolic regression relationship 22
Figure 5. The empirical relationship between average subsurface remote sensing reflectance (r_{rs}) in Landsat B4 and total suspended solids (TSS, mg L^{-1}). 23
Figure 6. The semi-analytical relationship between TSS concentrations as a function of the average of Landsat B3 subsurface remote sensing reflectance. A trigonometric relationship is used to approximate the semi-analytical relationship. This function was used to predict TSS concentration from B3 Landsat r_{rs}. 24
Figure 7. *In situ* TSS versus estimated TSS using the semi – analytical relationship with Landsat B3 24
Figure 8. Lake Waikare TSS estimated via. Eq. 10. Red open circles represent in situ TSS and blue open circles represent satellite estimated TSS. 25
Figure 9. Estimate of TSS in Lake Waikare on 22/07/2015, applying equation 12. 25
Figure 10. TSS estimations using Eq. 9 (left) and 10 (right). Red open circles represent in situ TSS and blue open circles represent satellite estimated TSS. 26
Figure 11. *In situ* chl *a* concentration as a function of chl end member fraction derived from linear spectral unmixing. 27
Figure 12. *In situ* vs. estimated chl *a* using linear spectral unmixing. 28
Figure 13 . Estimates chl *a* in Lake Waikato riverine lakes using linear spectral unmixing. . Red open circles represent in situ samples and blue open circles represent satellite estimated. 28
Figure 14. Estimates of chl *a* in relatively clear Waikato lakes using linear spectral unmixing. Red open circles represent in situ samples and blue open circles represent satellite estimated. 29
Figure 15. Chromaticity coordinates (x,y) for FWENZ lakes. The different colours of points within the plot represent FWENZ geomorphic classifications (black=aeolian, white=dam, red=geothermic, green=peat, blue=riverine, and yellow=volcanic). Note some volcanic lakes (yellow points) fall outside of the colour spectrum and these represent lakes with extreme reflectance. These lakes were also estimated as having very high TSS concentrations. Further research is needed to identify the reasons for these extremities in reflectance. Note that the colours displayed on this diagram are not identical to true colours. 30

List of tables

Table 1. *In situ* TSS data; site ID refers to the FWENZ unique identifier for each lake.....20
Table 2. Summary of models investigated in the present study to estimate TSS concentrations in the Waikato lakes.....26

Executive summary

This study explored and utilised existing remote sensing technology and algorithms to determine total suspended sediments (TSS) in lakes at a regional scale, producing a dataset quantifying spatial and temporal variability of remotely sensed TSS (including an experimental algorithm for chlorophyll *a* concentrations). The study processed Landsat 7 and 8 images from 1999 until the end of 2015. Statistical analysis included estimation of minimum, maximum, mean, range, and skewness of all Waikato lakes larger than 1 ha. The study demonstrated that the remote estimation of TSS within Waikato lakes is feasible and provides TSS estimations within the ranges of measured *in situ* TSS concentrations within most of the Waikato lakes except a small number of lakes with higher than expected estimated TSS concentrations (possible causes are identified including bottom reflection, and optical conditions not within the bounds of algorithm design). The study also demonstrated the ability of using remote sensing data to estimate and quantify variability of TSS over a large range of both within and between lakes. This spatial variation appeared to be driven by both geomorphic and abiotic factions, including turbid inflows and resuspension from the lakebed. The derived dataset maybe helpful to elucidate a better understanding of water quality variability and ultimately better understand implications for lake management. It is recommended that detailed *in situ* data be captured at the time of satellite overpass to further assess and improve the accuracy of the methods derived within the present study. The recent launch of Sentinel 2a (10 m resolution) will provide greater spatial and temporal coverage satellite imagery with a similar spectral resolution to Landsat 8 (30 m resolution) in the near future.

Introduction

Total suspended sediment (TSS) in aquatic ecosystems includes both organic and mineral fractions, and generally displays highly heterogeneous concentrations in shallow aquatic systems due to complex interactions of geomorphic, hydrodynamic and meteorological processes (e.g. erosion, transport, resuspension and circulation). Therefore, synoptic monitoring is generally required to estimate and quantify variability of TSS both within and between lakes. Suspended sediment attenuates light through scattering and absorption, and thereby plays a critical role in the determination of photic zone depth (Scheffer, 1998) and production of phytoplankton and macrophytes (Gallegos, 2001). Approaches to assess concentrations of TSS (and water quality generally) may be categorised broadly into three main types; point based *in situ* grab sampling, numerical modelling, remote sensing and remote monitoring. *In situ* methods using grab samples are generally suited to monitoring at low temporal resolution. By contrast autonomous water quality monitoring sensors allow for monitoring at high frequency and potentially in real time but often require ground-truthing (i.e. calibration of relative units measured by sensors). However, neither of these methods is well suited to effectively capturing the potential horizontal heterogeneity of water quality and temperature. Considering the critical role of TSS in regulating physical and biological properties of aquatic environments, it is essential to effectively monitor concentration. However, monitoring spatial heterogeneity using traditional grab samples can be inaccurate and/or costly. The application of remote sensing obviates the large cost of monitoring all aquatic systems within a region, and although there are limitations in terms of accuracy, useful water quality metrics can still be derived, including timing of algal bloom/turbidity events, broadening the general understanding of aquatic hydrodynamics and ecology. There is also potential for "hindcasting" water quality metrics using historical image archives.

Remote sensing can provide synoptic monitoring of water quality and temperature (e.g., Dekker et al., 2002; Kloiber et al., 2002), however limitations of this method must also be considered. Remote sensing using visible and infrared (IR) radiation is not possible during periods of extensive cloud cover, which are frequent in New Zealand. Remote sensing does also not allow direct estimates of non-optically active water constituents, such as nutrient concentrations. Measurements of total radiance from satellites may comprise up to 90% atmospheric path radiance, making it difficult to quantify radiance from optically active constituents of water (Vidot & Santer, 2005). Atmospheric correction is therefore essential for the standardisation of image time series. Waikato inland waters can be considered to fit that category of Case 2 due to bio-optics being function of at least three optically active constituents which can vary independently (Blondeau-Patissier et al., 2009). The retrieval of water constituent concentrations from Case 2 waters is more demanding in terms of algorithm complexity and the satellite sensor spectral resolution (Matthews, 2011). This is the case when using broadband sensors such as Landsat's Enhanced Thematic Mapper (ETM), accurate (or "fit for purpose") estimations of water quality in optically complex waters can be limited to more water quality variables that are constituent in nature, such as Secchi depth, light attenuation, and TSS.

In theory, subsurface remote sensing reflectance ($r_{rs}(\lambda)$) at visible and near infrared wavelengths is nearly linearly related to TSS at low to moderate concentrations. For high TSS, the relationship becomes non-linear, characterised by an asymptote where $r_{rs}(\lambda)$ becomes increasingly insensitive to rising in TSS concentrations (Bowers et al., 1998; Doxaran et al., 2002). This problem can be partly addressed by the use of wavelengths in the red and near infrared (NIR) regions (Ruddick et al., 2006). At NIR wavelengths, the

absorption by phytoplankton and coloured dissolved organic matter (CDOM) is minimal, and water dominates absorption relative to other optically active constituents. Therefore at NIR wavelengths the variation in $r_{rs}(\lambda)$ is primarily determined by changes in the scattering due to TSS (Ruddick et al., 2006).

Many empirical relationships have been developed to relate TSS to single-band wavelengths, especially in the red wavelengths (e.g., Kutser & Metsamaa, 2007; Nechad et al., 2010). For high concentrations of TSS (>2000 mg L^{-1}), reflectance ratios in red and NIR bands have been used to estimate TSS (Doxaran et al., 2009). A major limitation of empirically based models, however, is that satellite imagery needs to be calibrated concurrently with *in situ* data. Additionally, inaccuracies may occur when TSS concentrations are outside of those used for model calibration (Dekker et al., 2002) which is particularly true for empirical models. These inaccuracies can also cause by factors such as reflection from lake bottom sediments or macrophytes, or lakes with extreme reflectance values caused by absorption and scattering processes not accounted for with empirical or analytical techniques.

More advanced model algorithms such as linear mixture modelling (Tyler et al., 2006) and bio-optical modelling attempt to differentiate colour producing constituents. Bio-optical models have generally been applied to high spectral resolution satellite imagery such as that of MODIS, and to hyperspectral data, both of which allow precise measurement of spectral slopes. Broadband remote sensing instruments such as Landsat can record average slopes of both positive and negative values simultaneously as opposed to hyperspectral data (Bukata et al., 1995), but successful applications of bio-optical models for single water quality parameter retrieval exist where there are simple relationships between the colour producing constituent (TSS, chl *a* and CDOM) and reflectance. For example bio-optical models have been used to map suspended solid concentrations using Landsat and SPOT ('Satellite Pour l'Observation de la Terre' translated as "Satellite for Earth Observation") satellite data (Dekker et al., 2002). The advantage of bio-optical models is that *in situ* data not needed at the time of image capture, allowing for multi-site, multi-temporal and multi-sensor comparisons. Dekker et al. (2002) found that bio-optical algorithms for TSS produced a more reliable temporally robust algorithm. Their study also found random point samples within the synoptic predictions for TSS were on average within a mean value of ±20 to 30% of *in situ* grab samples, however, in the worst case scenario values differed by as much as 4000% (Dekker et al., 2002).

Objectives

The objective of this study was to explore and utilise existing remote sensing technology and algorithms to determine TSS in lakes at a regional scale. Specifically, this study aims at producing a dataset that can be used to quantifying spatial and temporal variability of remotely sensed TSS in these lakes (including an experimental algorithm for chlorophyll *a* concentrations). Such a dataset may ultimately be used for better describing the state of lakes over extended periods of time and to better understand drivers of temporal and spatial heterogeneity of a critical water quality parameter in these water bodies. This report describes remote sensing methods to derive the dataset of TSS in the Waikato lakes including the following tasks:

- Download archive of Landsat 8 and Landsat 7 imagery from 1999 until the end of 2015 (USGS atmospherically corrected) with, and TSS/turbidity estimated.

- Statistical analysis such as minimum, maximum, mean, range, and skewness of all Waikato lakes larger than 1 ha. Each lake name will be linked to the Fresh Water Environments of New Zealand (FENZ) database as a unique lake identification.
- Application of an experimental chlorophyll *a* index and semi quantitative estimation of chlorophyll *a* concentration.
- Results will be statistically compared to *in situ* measurements of TSS and chlorophyll *a* where data is available.
- Variation of watercolour will be investigated using chromaticity analysis.
- A scientific report will describe the methods (including a description of the study site), results, and discussion/conclusions.

Methods

The project proposes to use methods that have been documented within published literature to estimate TSS and chlorophyll *a* from Landsat satellite imagery. This will enable the quantification of water quality and lakes greater than 1 ha in size. This will include currently monitored lakes, and any other water bodies.

Waikato lakes study site

This study covers lakes in the Waikato region, which according to the Fresh Waters of National Importance (FWENZ) database (Leathwick et al., 2010) database includes 238 lakes, ponds or other standing water bodies ranging from 1 ha (unnamed water body) to 61264.5 ha Lake Taupo (Figure 1). There are 31 dystrophic (peat) lakes in the Waikato region, which are a remnant of the formerly extensive peat bogs of Komakorau, Rukuhia and Moanatuatua, forming the largest peat habitat in New Zealand. Peat lakes have classically been described as having low productivity, however, detailed investigations have shown that chl *a* is significantly higher in coloured lakes than clear lakes(Nurnberg & Shaw, 1998). Also, annual integral productivity of epilimnetic bacterioplankton has also been found to be much higher in peat lakes than in clear water lakes (Nurnberg & Shaw, 1998). An anoxic hypolimnia is common in peat lakes due to decomposition of organic carbon (Wetzel, 2001). Peat lakes are typically brownish due to high levels of DOM leached from surrounding peat lands, and are generally mildly acidic (pH 5.5 – 6.5).

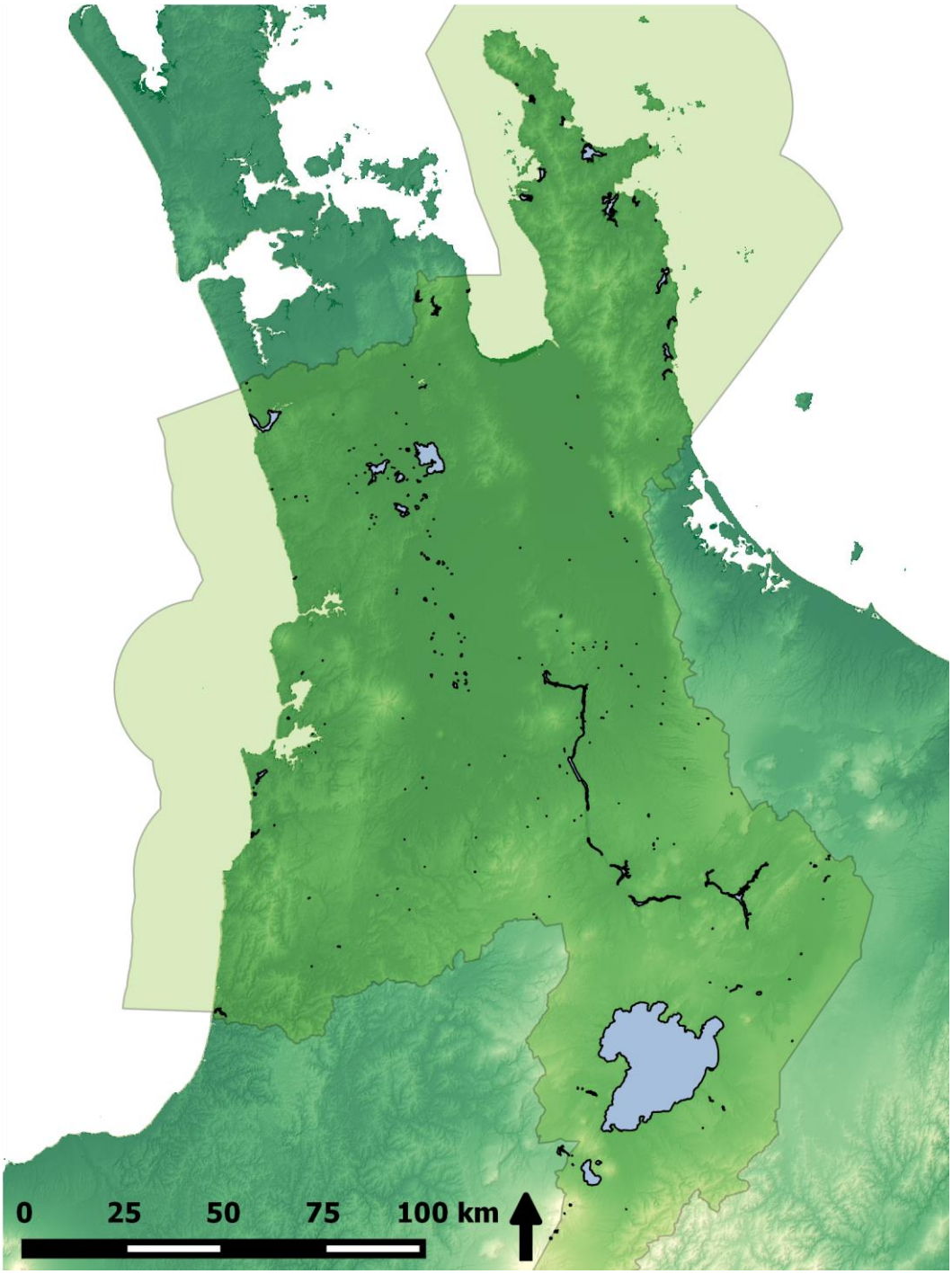

Figure 1. Waikato study site map including lakes and estuaries

The larger riverine lakes in this study include lakes Waikare and Waahi, which were formed when alluvial deposits diverted the original path of the Waikato River, damming valleys and tributaries. Lake Waikare is a large shallow hyper-eutrophic lake characterized by extremely high levels of inorganic suspended sediment. This sediment may be attributed to erosion from the Matahuru catchment and from resuspension from the lakebed by wave action. The high TSS concentrations found here are thought to be the principal factor controlling productivity in the lake, limiting light penetration and hence phytoplankton growth (Barnes, 2002). The TSS in Lake Waikare consists mainly of clay particles which are easily resuspended, keeping

the lake in a constant turbid state even during periods of stable weather (Stephens et al., 2004).

Lake Whangape is the second largest riverine lake in the Waikato region. It is a shallow hyper-eutrophic lake with an average depth of 1.5 m. During summer the lake has weak thermal stratification with oxygen depletion in deeper waters (Boswell et al., 1985). The lake catchment is consisted of mainly agricultural land, but in the past, the lake has received inputs from mining activities (Barnes, 2002). This lake suffered an *Egeria densa* macrophyte collapse in 1987 (Champion et al., 1993). This has been attributed to a number of factors including phytoplankton blooms, grazing from pest fish, cultural eutrophication, and increase in inorganic sediment levels (Wells et al., 1988). Vant, (1987) attributed the macrophyte collapse to discharge of inorganic sediment in mining wastewater.

Lake Waahi is a relatively shallow super-eutrophic lake dominated by high turbidity and high algal biomass since the macrophyte collapse in the late 1970s, which was attributed to low lake levels, high nutrient concentrations, and continued sediment input from mining (Dell, 1988).

Lake Rotomanuka North is a small eutrophic peat lake remnant of the once larger Lake Rotomanuka, the past lake bed forming the surrounding wetland (10 ha) that connects to Lake Gin (Rotomanuka South). The catchment is comprised of intensive dairy and pastoral farming. The decrease in water clarity, increase in total nitrogen and total phosphorus could be attributed to the collapse of macrophyte beds that occurred in 1996/1997, where the input of detritus and following microbial decomposition nutrients released organic nitrogen and phosphorus, which for some reason remains unavailable (Barnes, 2002). Furthermore, little seasonality was observed in water quality parameters (Barnes, 2002) although stratification and bottom anoxia has been recorded in summer months (Boswell et al., 1985).

Remote sensing

Satellite imagery, software and in situ data

USGS on demand atmospherically corrected Landsat imagery was ordered from http://espa.cr.usgs.gov/index/. Atmospheric correction applies the radiative transfer model 6sv (Second Simulation of a Satellite Signal in the Solar Spectrum), which corrects for atmospheric scattering and absorption effects of gases, and aerosols (Kotchenova et al., 2008). Landsat 7 and 8 satellite images were captured between 1999 and 2015. All image processing routines were automated using scripts written in Interactive Data Language (IDL). Maps of derived TSS outputs were generated using Quantum GIS (QGIS). For the purpose of this study all available Landsat 7 and 8 images were downloaded (235 images) from Landsat path/row 072/087 (84 L7, 17 L8) and 073/086 (118 Landsat 7, 16 L8). Lake polygons were sourced from FENZ (Freshwater Environments of New Zealand, Leathwick et al. (2010)), which include a unique lake ID (LID). Statistics were calculated from the whole lake (excluding a 30 m buffer zone from shoreline polygon), lake centroid (real centroid plugin in Quantume GIS (QGIS), and from 2x2 pixel area of interest surrounding WRC lake water quality monitoring sites. In situ TSS and chl *a* were collected by WRC.

TSS was estimated from Landsat subsurface remote sensing reflectance using both empirical and semi-analytical algorithms similar to those found in Allan et al. (2015) and

Dekker et al. (2002). Forward bio-optical modelling was used to quantify the physical processes responsible for relationships between Landsat measured reflectance and TSS concentrations. These relationships were used to predict TSS from inverted reflectance. The relationship between $r_{rs}(\lambda)$ and the total backscattering coefficient b_b (m^{-1}) and total absorption a (m^{-1}) is (Gordon et al., 1988):

$$r_{rs}(\lambda) = g_0 u(\lambda) + g_1 [u(\lambda)]^2 \quad (1)$$

where u is defined as (Dekker et al., 1997):

$$u(\lambda) = \frac{b_b(\lambda)}{a(\lambda) + b_b(\lambda)} \quad (2)$$

and g_o and g_1 are empirical constants that depend on the anisotropy of the downwelling light field and scattering processes within the water. The constant g_o is equivalent to f/Q where f represents geometrical light factors and Q represents the light distribution factor, which is defined as upwelling subsurface irradiance/upwelling subsurface radiance) (Maritorena et al., 2002).

The absorption and backscattering coefficients are comprised of individual optically active constituents:

$$b_b(\lambda) = b_{bw}(\lambda) + B_{bSP}\, b^*_{SP}(\lambda)\, C_{SP} \quad (3)$$

$$a(\lambda) = a_w(\lambda) + C_\phi\, a^*_\phi(\lambda) + a_{CDOMD}(\lambda) \quad (4)$$

$$a_{CDOMD}(\lambda) = a_{CDOMD}(\lambda_{440}) \exp[-S\,(\lambda - \lambda_{440})] \quad (5)$$

where:
$b_{bw}(\lambda)$ = backscattering coefficient of water,
B_{pSP} = backscattering ratio from SP,
$b^*_{SP}(\lambda)$ = specific scattering coefficient of SP,
C_{SP} = concentration of SP,
$b^*_\phi(\lambda)$ = specific scattering coefficient of phytoplankton,
$a_w(\lambda)$ = absorption coefficient of pure water,
C_ϕ = concentration of chl *a*,
$a^*_\phi(\lambda)$ = specific absorption coefficient of phytoplankton,
$a_{CDOMD}(\lambda)$ = absorption coefficient for coloured dissolved organic matter (CDOM),
S = spectral slope coefficient

Values of $a_w(\lambda)$ and $b_{bw}(\lambda)$ were prescribed from the literature (Pope & Fry, 1997). The backscattering ratio of SP, B_{pSP}, was set to 0.01. The specific scattering coefficient of SP at the Landsat b3 wavelength was estimated using a power function (Morel & Prieur, 1977):

$$b^*_{SP}(\lambda) = b^*_{SP}(555)\left(\frac{555}{\lambda}\right)^n \quad (6)$$

where the value $b^*_{SP}(555)$ was set to 0.6 m^2 g^{-1}. The hyperbolic exponent n was set to 0.63, equating to a value measured in Lake Taupo, New Zealand (Belzile et al., 2004). The specific absorption coefficient of phytoplankton $a^*_\phi(662)$ was 0.0136 m^2 mg^{-1} , equal to the average value measured in eight Dutch lakes (Dekker et al., 2002). The bio-optical simulations were run by varying SP concentration from 0.1 to 417.6 mg L^{-1} in increments of 0.5 mg L^{-1} while $a_{CDOMD(440)}$ was fixed at 0.1 m^{-1} with chl *a* (µg L^{-1}) taken to increase with TSS (chl *a*= TSS/20) ranging from 0.03 to 110 µg L^{-1}.

Linear spectral unmixing

Spectral unmixing is an inversion technique that aims at estimating the mixture components responsible for the mixed spectral signature of a pixel, defined as a linear-matrix equation:

$$R_i = \sum_{k=n}^{n} f_k R_{ik} + \varepsilon_i \qquad (7)$$

where R_i is the reflectance of the mixed pixel for each band *i*, including one or more endmembers; f_k is the fraction of each endmember *k* within the pixel, R_{ik} is the reflectance of the endmember *k* within the pixel on band *i*, and ε_i is the error for band *i* (or the difference between the measured and modelled DN in each band).

To solve these equations, the endmembers must be independent from each other, the number of endmembers should be less than or equal to the number of spectral bands used, and the spectral bands used should not be highly correlated.

The water surface reflection received by satellites is a mixed spectrum as it is affected by chl *a*, SS, DOM concentrations, as well as other factors. LSU attempts to unmix this signature, deriving proportion estimates of the mixture components. These mixture components are referred to as endmembers, which are idealized pure signatures. In this study, an image based endmember selection process was used where bands are plotted in feature space, and endmembers identified manually using a similar approach to Tyler et al. (2006). Spectrally pure endmembers are found at the vertices of the polygon bounding the data cloud in feature space.

Watercolour

Landsat chromaticity coordinates were derived from the x and y components of International Commission on Illumination (CIE) XYZ colour space (Appendix 1), applied using Matlab scripts (Westland & Ripamonti, 2004):

$$x=X/(X+Y+Z),\ y=(Y/(X+Y+Z) \qquad (8)$$

where are XYZ CIE primaries are substituted for Landsat bands of red, blue and green atmospherically corrected reflectance respectively. Using the derived x and y components a chromaticity diagram was be plotted in order to map colour space. CIE LAB colour was also calculated from XYZ. LAB is a three-dimensional colour space where the a and b axes form one plane and the lightness L axis is orthogonal to this plane. The dominant wavelength was

calculated by a Matlab script, which draws a line between a reference white point and the chromaticity coordinates of the Landsat sample. The line is extrapolated until it meets a locus representing spectrally pure colours. The pixel purity is then calculated as the ratio of the length of the line segment that connects the chromaticity coordinates of the reference white point and the length of line that connects the white point to the dominant wavelength (at the locus).

Results

Total suspended solids (TSS)

A total of 24 *in situ* samples of TSS were available on the same day as the 235 L7 and L8 images were taken (after exclusion of cloud and cloud shadow satellite data) with *in situ* TSS ranging from 2 to 240 mg L^{-1} (Table 1) for the period between 1999 and 2015.

Table 1. *In situ* TSS data; site ID refers to the FWENZ unique identifier for each lake

Date	Site ID	Lake name	Station name	*In situ* TSS (mg L^{-1})
26/10/2012	330_14	Lake Whangape	Centre (Surface)	126
28/08/2002	330_14	Lake Whangape	Centre (Surface)	47
28/08/2002	324_11	Lake Waahi	Weavers Basin (Surface)	15
26/10/2012	326_4	Lake Waikare	Epilimnion	108
14/03/2011	326_2	Lake Waikare	Centre-Surface	19
30/05/2013	317_4	Lake Rotomanuka	Lake Centre (Surface)	5
30/05/2013	301_8	Lake Maratoto	Centre (Surface)	2
28/08/2002	324_2	Lake Waahi	Centre (Surface)	17
28/08/2002	326_4	Lake Waikare	Epilimnion	219
14/03/2011	324_2	Lake Waahi	Centre (Surface)	75
14/03/2011	292_6	Lake Hakanoa	Centre (Surface)	16
23/04/2014	330_14	Lake Whangape	Centre (Surface)	74
29/10/2007	292_6	Lake Hakanoa	Centre (Surface)	25
30/05/2013	1456_3	Lake Serpentine	North (Surface)	2
28/05/2015	317_4	Lake Rotomanuka	Lake Centre (Surface)	5
28/05/2015	301_8	Lake Maratoto	Centre (Surface)	3
6/03/2014	290_2	Lake Areare	Centre-Surface	6
23/04/2014	292_6	Lake Hakanoa	Centre (Surface)	20
28/08/2008	1456_3	Lake Serpentine	North (Surface)	4.4
23/04/2014	326_4	Lake Waikare	Epilimnion	118
28/05/2015	1456_3	Lake Serpentine	North (Surface)	4
23/04/2014	2069_1	Lake Puketirini (Lak	Centre (Surface)	2
23/04/2014	324_2	Lake Waahi	Centre (Surface)	240
6/03/2014	299_1	Lake Mangakaware	Lake Centre	12

Previous studies have found Landsat B2 B3 average reflectance was best suited for TSS concentration estimation (Dekker et al., 2002). Applying a second order polynomial fit, the r^2 between *in situ* TSS and average Landsat $B2B3r_{rs}$ was 0.68 (Fig. 2), with RMSE of TSS estimation of 37.59 mg L^{-1} (Fig. 3):

$$TSS = 54540\ B2B3r_{rs}^{\ 2} + 290.02\ B2B3r_{rs} - 1.87 \quad (9)$$

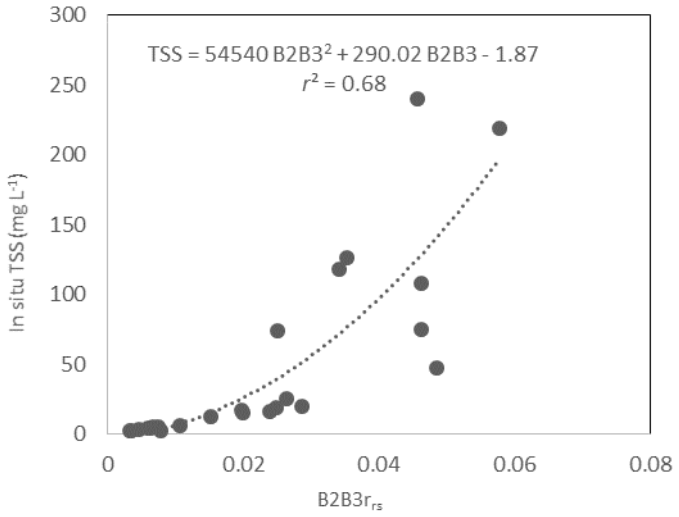

Figure 2. The empirical relationship between average subsurface remote sensing reflectance (r_{rs}) in Landsat B2B3 and total suspended solids (TSS, mg L^{-1}).

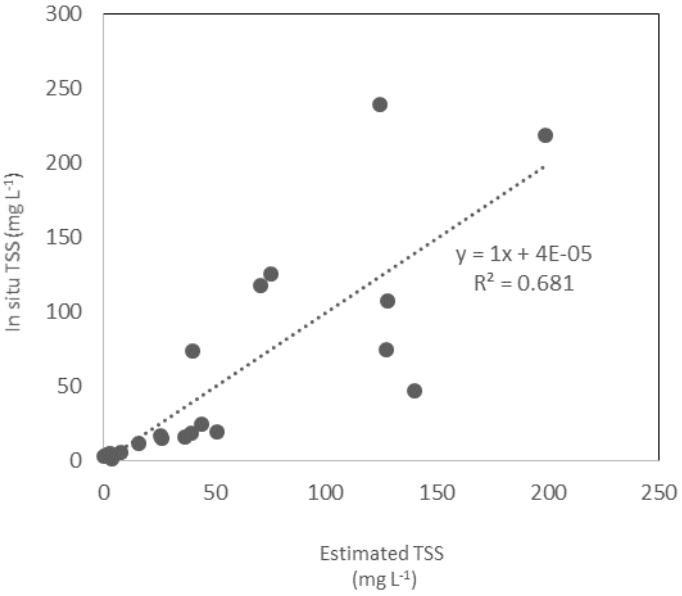

Figure 3. *In situ* TSS versus estimated TSS using the empirical relationship between average subsurface remote sensing reflectance (r_{rs}) in Landsat B2B3 and total suspended solids (TSS, mg L^{-1}).

Symbolic regression was also applied to investigate the relationship between remote sensing reflectance and *in situ* TSS and the following simple relationship was found:

$$TSS = 22983.65\ B3\ B4 \qquad (10)$$

The application of this relationship to estimate TSS resulted r^2 0.87, and a RMSE 25.5 mg L^{-1} (Fig. 4).

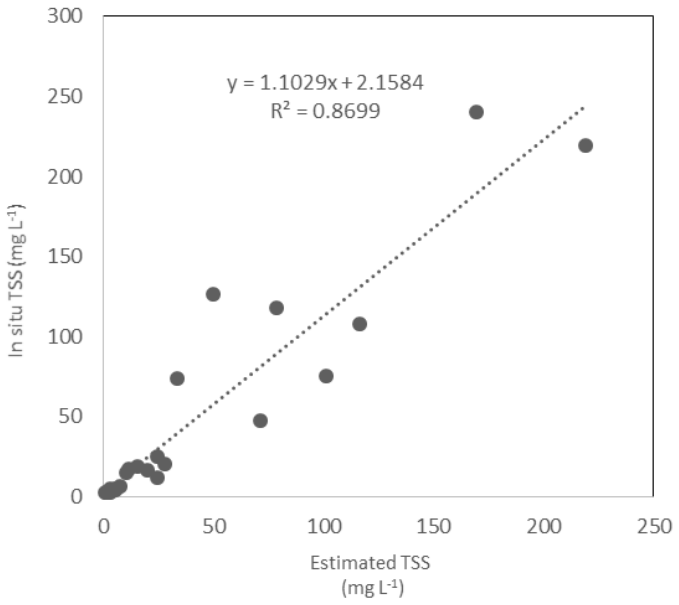

Figure 4. ***In situ*** **TSS versus estimated TSS using symbolic regression relationship**

Landsat Band 4 has previously been used to estimate TSS in the Waikato lakes (Hicks et al., 2013) using a linear relationship between *in situ* data (n =36) captured within three days of satellite overpass. In the case of the present study this relationship was found to be non-linear. Using *in situ* data captured on the day of satellite overpass, applying a second order polynomial fit, the coefficient of determination between *in situ* TSS and average Landsat $B4r_{rs}$ was 0.89 (Fig. 5), with RMSE of TSS estimation of 34.4 mg L^{-1}:

$$TSS = 72678\ B4^2 + 1020\ B4 - 11.317 \quad (11)$$

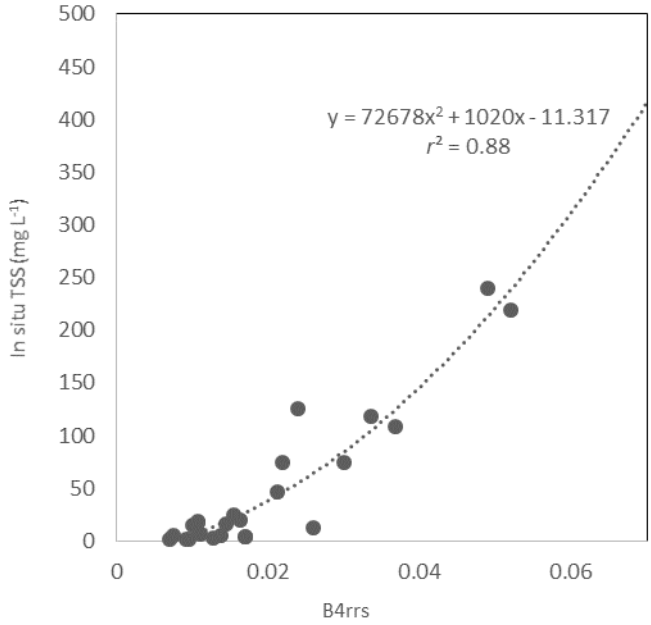

Figure 5. The empirical relationship between average subsurface remote sensing reflectance (r_{rs}) in Landsat B4 and total suspended solids (TSS, mg L^{-1}).

The semi-analytical relationship between TSS and $B3r_{rs}$ (modelling procedure described in methods) was approximated using trigonometric relationship with r^2 of 1. This relationship was also used to estimate TSS concentrations from observed Landsat $B3r_{rs}$ (Fig. 6), and application of this equation resulted r^2 0.67 and RMSE of 38.4 between observed and estimated TSS (Fig. 7).

$$TSS = 6.71 - 986.0\ B3 \tan(12 - 13.13\ B3) \quad (12)$$

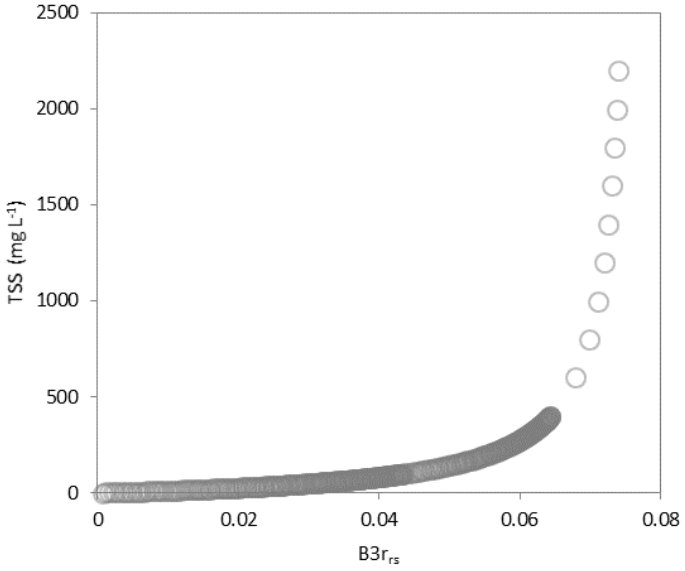

Figure 6. The semi-analytical relationship between TSS concentrations as a function of the average of Landsat B3 subsurface remote sensing reflectance. A trigonometric relationship is used to approximate the semi-analytical relationship. This function was used to predict TSS concentration from B3 Landsat r_{rs}.

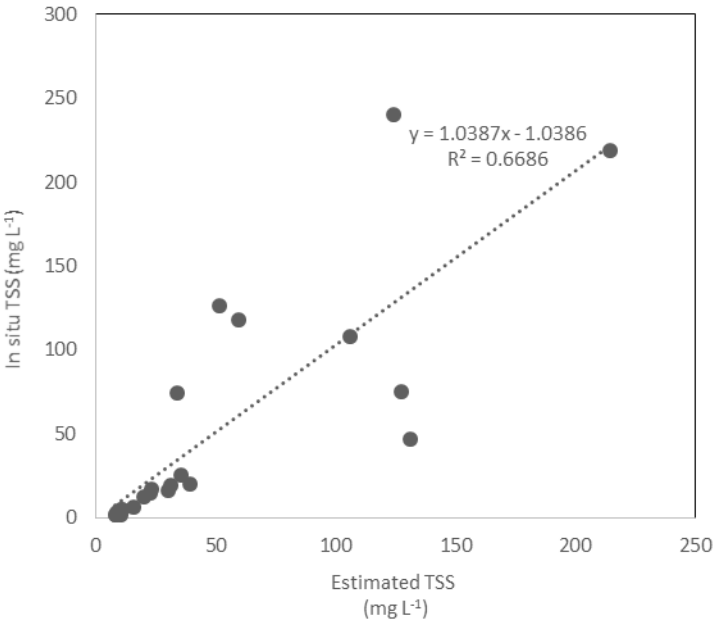

Figure 7. *In situ* TSS versus estimated TSS using the semi – analytical relationship with Landsat B3

Equation 10 was applied all currently monitored WRC surface lake water quality sites (141 sites within 49 lakes after cloud and land masking) to estimate TSS for all satellite overpass dates, and time series estimations of TSS were created which corresponded to a 2 x 2 cell area of interest surrounding WRC sampling locations. For example, time series estimations of TSS in Lake Waikare were highly temporally and spatially variable (Fig. 8 and 9). This is also demonstrated in a time series visualization (Appendix folder 1).

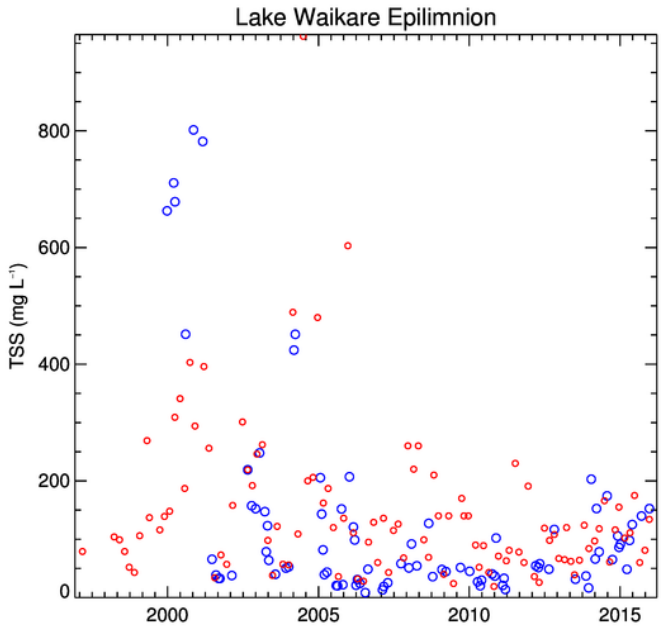

Figure 8. Lake Waikare TSS estimated via. Eq. 10. Red open circles represent in situ TSS and blue open circles represent satellite estimated TSS.

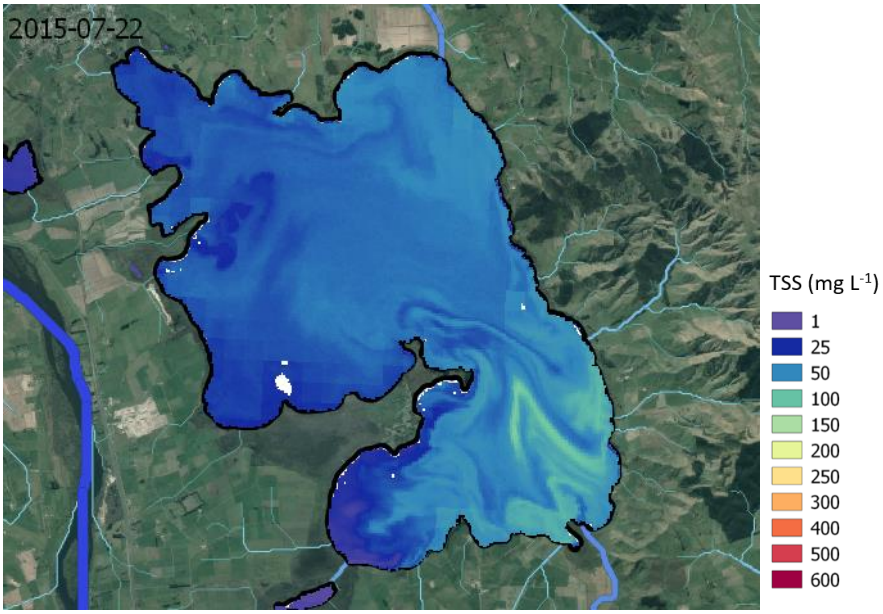

Figure 9. Estimate of TSS in Lake Waikare on 22/07/2015, applying equation 12.

For turbid Waikato riverine lakes, time series estimations from Eq.s 9-12 were comparable, however for relatively clear lakes such as lakes Puketirini and Taharoa, there were large variations in the magnitude of TSS estimations and likely overestimation in most cases (e.g. Fig 10). However equation 10 (symbolic regression using B3 B4) resulted in potentially less over estimation (Fig. 10).

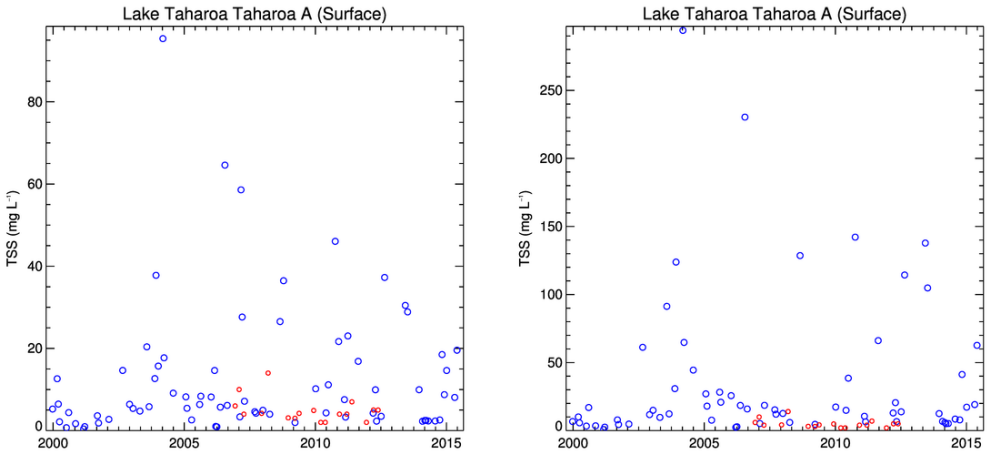

Figure 10. TSS estimations using Eq. 9 (left) and 10 (right). Red open circles represent in situ TSS and blue open circles represent satellite estimated TSS.

Table 2. Summary of models investigated in the present study to estimate TSS concentrations in the Waikato lakes.

Equation number in text	Equation	Type of relationship	R^2	RMSE (mg L^{-1})
9	TSS = 54540 B2B3$r_{rs}{}^2$ + 290.02 B2B3r_{rs} - 1.87	Second order polynomial	0.68	37.59
10	TSS= 22983.65 B3 B4	Symbolic regression	0.87	25.5
11	TSS = 72678 $B4^2$ + 1020 B4 - 11.317	Linear relationship	0.89	34.4
12	TSS = 6.71 - 986.0 B3 tan(12 - 13.13 B3)	Semi-analytical relationship	0.67	38.4

The TSS estimations derived from Eq. 10 was also applied to estimate TSS (excluding a 30 m buffer zone from the shoreline) within FWENZ lakes within the WRC territorial authority and within Landsat data capture zone (Appendix table 1). This included data from 188 lakes/ponds or dams (Lake Puketirini was missing from FWENZ, but was added to this analysis). Some of the TSS estimations from these lakes was only retrieved in a few instances, due to the small size of the lakes, and the greater majority of samples being flagged as land. The number of successful retrievals of TSS concentrations within these lakes ranged from 1 (six unnamed water bodies) to 221 (lakes Karapiro and Arapuni, which lie within both Landsat scenes analysed during the study). It should be noted here that the 30 m buffer zone exclusion from the lake edge does not necessarily preclude lake bottom reflection (potentially causing erroneously high/low estimation of TSS). For example in Lake Taupo edge effects/bottom effects have the potential to cause erroneously high estimations in up to 1.5 km from the lake shoreline.

The spatial variation of TSS concentrations within each lake varied greatly both within and between lakes. The average difference between lake wide mean TSS and lakes centroid (approximate lake centre) TSS gives an indication of within lake spatial variation. Lake Taupo had the lowest estimated difference between lake centroid and whole lake TSS (0.05 mg L^{-1}), with large turbid riverine lakes possessing greater differences (e.g. Whangape 15.06 mg L^{-1}). Note here that any errors associated with bottom reflection contribute to centroid average TSS.

Chlorophyll *a*

For the estimation of chl *a* concentrations in WRC lakes, linear spectral unmixing was applied. The relationship between chl endmember and *in situ* chl *a* (n=22) resulted in an r^2 of 0.23:

In situ chl *a* = 75.59 chl_endmember + 17.70 (13)

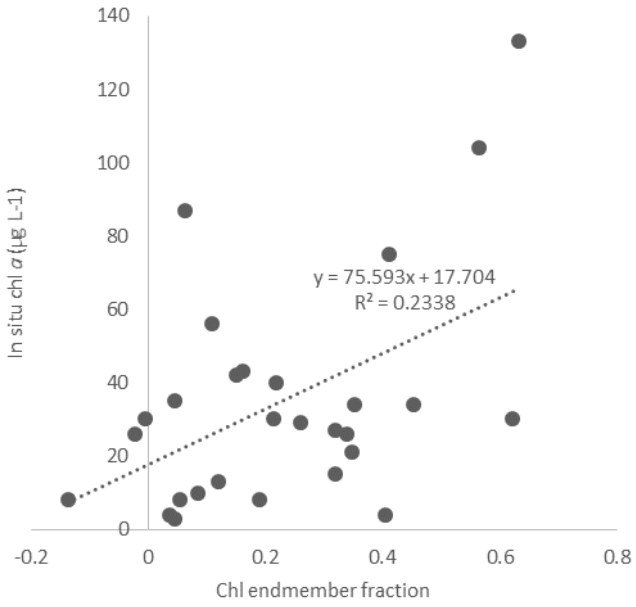

Figure 11. *In situ* chl *a* concentration as a function of chl end member fraction derived from linear spectral unmixing.

A polynomial based symbolic regression derived relationship was used to estimate chl *a* concentration, and observed vs. estimated chl *a* resulted in an r^2 of 0.34, and RMSE of 27.4 µg L^{-1} (Fig 12):

Chl *a* = 2.17 + 508.43 $chl_endmember^3$ - 163.46 $chl_endmember^4$ (14)

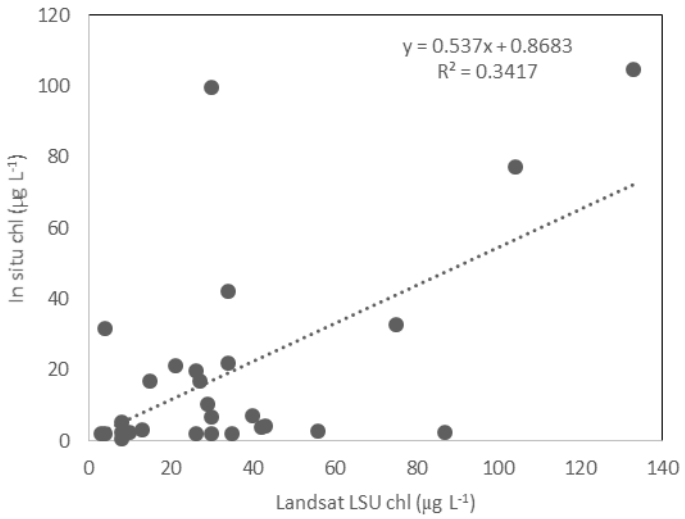

Figure 12. *In situ* vs. estimated chl *a* using linear spectral unmixing.

While the algorithm does not appear to perform well in chl *a* estimation when compared to the field data, comparison of time series estimated chl *a* shows promise in turbid lakes. For example, the range of estimated chl *a* in Lakes Waikare, Waahi and Whangape is comparable to *in situ* values (Fig 13).

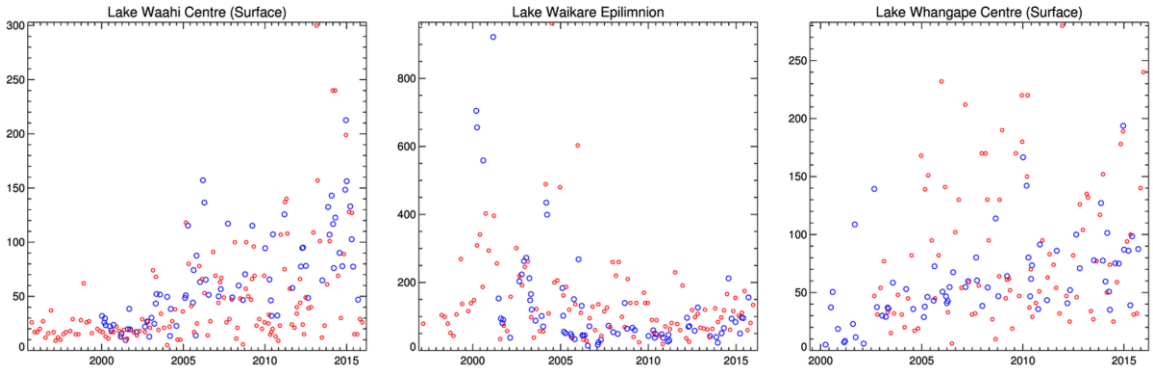

Figure 13 . Estimates chl *a* in Lake Waikato riverine lakes using linear spectral unmixing. . Red open circles represent in situ samples and blue open circles represent satellite estimated.

However, within relatively clear lakes chl *a* estimations were not within measured ranges (Fig. 14).

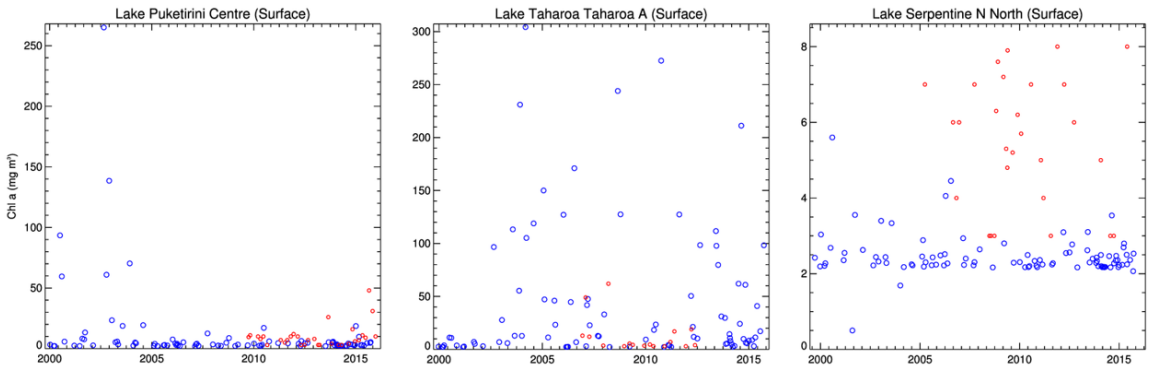

Figure 14. Estimates of chl *a* in relatively clear Waikato lakes using linear spectral unmixing. Red open circles represent in situ samples and blue open circles represent satellite estimated.

Chromaticity analysis

The chromaticity analysis Waikato lakes watercolour revealed a broad range of watercolours displayed by geomorphic lake types in the study area (Fig. 15). Volcanic lakes were in some instances similar to other geomorphic lake types, however there was a tendency for retrieved reflectance to display a dominant wavelength at blue regions of the spectrum (Appendix table 2). In some instances these outlier lakes had very high estimations of TSS concentrations. For example a very small 1 ha unnamed volcanic lake (ID 20852) had the lowest average dominant wavelength, and very high estimations of TSS. Chromaticity coordinates revealed an average reflectance that was spectrally flat (average x , y, z similar). Visual analysis of the lake shows a light brown hue, which indicates high TSS concentrations may be present. FWENZ ID 20853 also displayed a spectrally flat reflectance and very high estimations of TSS, and visual analysis shows a yellow/brown hue, also indicative of very high TSS, with potential bottom reflectance in shallow areas. Blue lake (FWENZ ID 20853) has a bright milky blue colour, potentially indicating the presences of fine strongly scattering sediment.

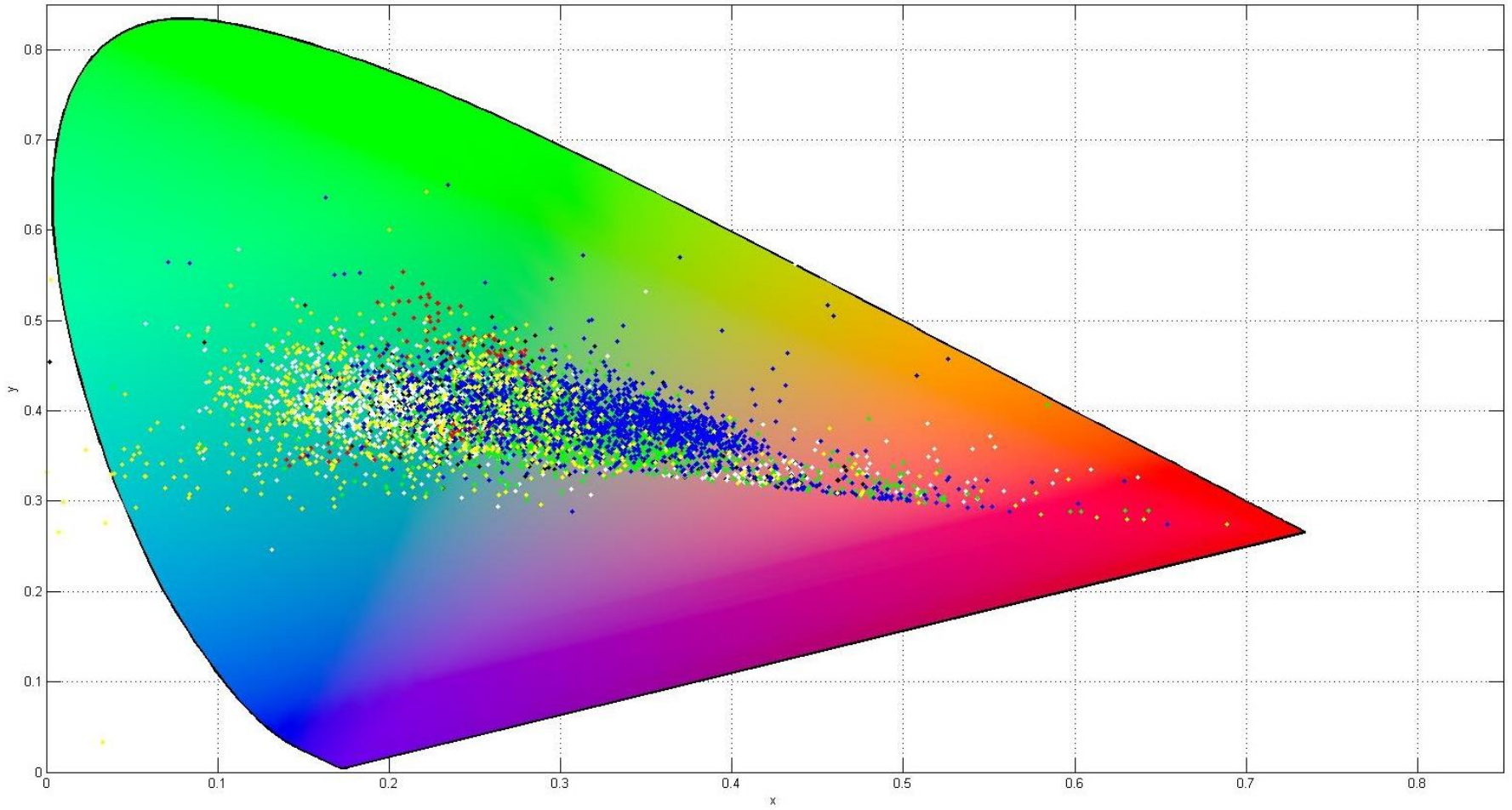

Figure 15. Chromaticity coordinates (x,y) for FWENZ lakes. The different colours of points within the plot represent FWENZ geomorphic classifications (black=aeolian, white=dam, red=geothermic, green=peat, blue=riverine, and yellow=volcanic). Note some volcanic lakes (yellow points) fall outside of the colour spectrum and these represent lakes with extreme reflectance. These lakes were also estimated as having very high TSS concentrations. Further research is needed to identify the reasons for these extremities in reflectance. Note that the colours displayed on this diagram are not identical to true colours.

Discussion

The present study demonstrated the ability of remote sensing to quantify TSS concentrations in lakes and displayed a large estimated range, both within and between lakes. This spatial variation appeared to be driven by both geomorphic and abiotic factions, including turbid inflows and resuspension from the lake bed. The large estimated difference between lake centroid and lake mean TSS showed by the study provides an effective method to quantify the spatial variation. This study demonstrated that the remote estimation of TSS within Waikato lakes is feasible and provides TSS estimations within the ranges of measured *in situ* TSS concentrations within most of the Waikato lakes. However, there are exceptions with possible high errors in estimations of TSS concentrations. This is likely caused by the unique inherent optical properties in some volcanic and riverine lakes, which were outside the range determined by the empirical algorithms within the study. In order to estimate TSS within these lakes *in situ* inherent optical property data may be needed alongside TSS estimations at or near the date of the satellite overpass, similar to those measured within Lake Pukaki (Gallegos et al., 2008). In addition, the influence of lake benthic sediment reflections can produce erroneous estimates of TSS must be considered in some clear lakes.

The higher r^2 produced using the symbolic regression TSS estimation (see Eq. 12) may be explained due to the addition of both Landsat B3 (red) and B4 (NIR). The use of both red and NIR wavelengths has been previously shown to minimize the influence of CDOM absorption at these wavelengths. In addition at NIR wavelengths the absorption from chloroform is also minimized (Ruddick et al., 2006). While remote sensing reflectance algorithms were shown to explain up to 86% of variation of TSS concentrations within the present study, other studies have shown the ability of Landsat to explain much more variation (e.g. Allan 2008 over Waikato lakes r^2 of 0.98, n=15). For example within lakes Wairarapa and Onoke the relationship between observed and estimated TSS using Landsat B3 based algorithm produced an r^2 of 0.97, RMSE 16.62 mg L^{-1}, and 32% RMSE, over a range of *in situ* TSS from 3 - 239 mg L^{-1}. Numerous factors have potential to decrease the accuracy or percent variation explained of *in situ* TSS from remote sensing data. These factors include temporal mismatch between the time of image capture and the time of *in situ* sampling, especially within turbid lakes susceptible to sediment resuspension due to wind initiated currents. In addition spatial miss match between *in situ* grab sample (representative of a very small area) and Landsat based area of interest (3600 m^2) may also influence errors. Therefore the "error" in TSS estimation is not only algorithm based but also can include sampling bias.

The final derived algorithm applied for Landsat based TSS estimation within the present study is relatively simple and represents less feasibility restraints for information within regional councils than previous algorithms. The use of atmospherically corrected data obviates this often complicated processing step. However the method still requires the user to have significant remote sensing experience and be able to run and manipulate script based processing routines. However someone with GIS experience (even with little scripting background) could be trained to apply this algorithm using the scripts generated for IDL.

Conclusions

The results obtained during this study have potential to be used for determining spatial and temporal variation of an important water quality attribute in inland waters, which may then be used, for example, to inform the design of monitoring networks. In particular, the within lake spatial variation of water quality in larger lakes implies that multiple *in situ* monitoring points may be required to fully capture spatial heterogeneity representatively.

The derived dataset maybe helpful to elucidate a better understanding of water quality variability and ultimately better understand implications for lake management. For example, use of the dataset to analyze potential drivers of water quality such as lake morphology, climate, and anthropogenic influences and the interactive effects with, for example, different land-use types at regional scale.

It is recommended that detailed *in situ* data be captured at the time of satellite overpass to further assess and improve the accuracy of the methods derived within the present study. The recent launch of Sentinel 2a (10 m resolution) will provide greater spatial and temporal coverage satellite imagery with a similar spectral resolution to Landsat 8 (30 m resolution) in the near future.

References

Allan, M. G., Hamilton, D. P., Hicks, B., & Brabyn, L. (2015). Empirical and semi-analytical chlorophyll a algorithms for multi-temporal monitoring of New Zealand lakes using Landsat. *Environmental Monitoring and Assessment*, *187*(6). http://doi.org/10.1007/s10661-015-4585-4

Barnes, G. (2002). Water Quality Trends in Selected Shallow Lakes in the Waikato Region , 1995-2001. *Environment*, (July), 1995–2001. http://doi.org/ISSN: 1172-4005

Belzile, C., Vincent, W. F., Howard-Williams, C., Hawes, I., James, M. R., Kumagai, M., & Roesler, C. S. (2004). Relationships between spectral optical properties and optically active substances in a clear oligotrophic lake. *Water Resources Research*, *40*(12), W12512. Retrieved from http://www.cen.ulaval.ca/warwickvincent/PDFfiles/184.pdf

Blondeau-Patissier, D., Brando, V. E., Oubelkheir, K., Dekker, A. G., Clementson, L. A., & Daniel, P. (2009). Bio-optical variability of the absorption and scattering properties of the Queensland inshore and reef waters, Australia. *Journal of Geophysical Research*, *114*(C5), C05003. http://doi.org/10.1029/2008JC005039

Boswell, J.; Russ, M.; Simons, M. J. (1985). *Waikato small lakes: resource statement*. Waikato Valley Authority. Technical report no.1985/7.

Bowers, D. G., Boudjelas, S., & Harker, G. E. L. (1998). The distribution of fine suspended sediments in the surface waters of the Irish Sea and its relation to tidal stirring. *International Journal of Remote Sensing*, *19*, 2789–2805.

Bukata, R. P., Jerome, J. H., Kondratyev, K. Y., & Pozdnyakov, D. V. (1995). *Optical properties and remote sensing of inland and coastal waters*. Boca Raton, Florida: CRC Press, Boca Raton, Florida, USA.

Champion, P.D.; de Winton, M.D.; de Lange, P. J. (1993). *The vegetation of the lower Waikato lakes. Volume 2. Vegetation of thirty-eight lakes in the lower Waikato. NIWA Ecosystems publication No.8. National Institute of Water and Atmospheric Research.*

Dekker, A. G., Vos, R. J., & Peters, S. W. M. (2002). Analytical algorithms for lake water TSM estimation for retrospective analyses of TM and SPOT sensor data. *International Journal of Remote Sensing*, *23*(1), 15–35. Retrieved from http://www.informaworld.com/10.1080/01431160010006917

Dell, P. (1988). *Lake Waahi catchment water and soil management plan.* Waikato Catchment Board Technical Publication Number 56.

Doxaran, D., Froidefond, J., Lavender, S., & Castaing, P. (2002). Spectral signature of highly turbid waters Application with SPOT data to quantify suspended particulate matter concentrations. *Remote Sensing of Environment*, *81*, 149–161.

Gallegos, C. L. (2001). Calculating Optical Water Quality Targets to Restore and Protect Submersed Aquatic Vegetation : Overcoming Problems in Partitioning the Diffuse Attenuation Coefficient for Photosynthetically Active Radiation. *Estuaries*, *24*(3), 381–397.

Gallegos, C. L., Davies-Colley, R. J., & Gall, M. (2008). Optical closure in lakes with contrasting extremes of reflectance. *Limnology and Oceanography*, *53*(5), 2021–2034. http://doi.org/10.4319/lo.2008.53.5.2021

Hicks, B. J., Stichbury, G. a, Brabyn, L. K., Allan, M. G., & Ashraf, S. (2013). Hindcasting water clarity from Landsat satellite images of unmonitored shallow lakes in the Waikato region, New Zealand. *Environmental Monitoring and Assessment*. http://doi.org/10.1007/s10661-013-3098-2

Kloiber, S. M., Brezonik, P. L., & Bauer, M. E. (2002). Application of Landsat imagery to regional-scale assessments of lake clarity. *Water Research*, *36*(17), 4330–4340. Retrieved from http://www.sciencedirect.com/science/article/B6V73-4607Y74-6/2/fe3f573e1aa1387d2877359da4960ef3

Kotchenova, S. Y., Vermote, E. F., Levy, R., & Lyapustin, A. (2008). Radiative transfer codes for atmospheric correction and aerosol retrieval: intercomparison study. *Applied Optics*, *47*(13), 2215–2226. Retrieved from http://www.ncbi.nlm.nih.gov/pubmed/18449285

Kutser, T., & Metsamaa, L. (2007). Operative monitoring of the extent of dredging plumes in coastal ecosystems using MODIS satellite imagery. *Journal of Coastal Research*, *SI 50*, 180–184. Retrieved from http://www.griffith.edu.au/conference/ics2007/pdf/ICS035.pdf

Leathwick, J. R., West, D., Gerbeaux, P., Kelly, D., Robertson, H., Brown, D., … Ausseil, A.-G.

(2010). Freshwater Ecosystems of New Zealand (FENZ) Geodatabase: User Guide., 51.
Matthews, M. (2011). A current review of empirical procedures of remote sensing in inland and near-coastal transitional waters. *International Journal of Remote Sensing*, *32*, 6855–6899.
Morel, A., & Prieur, L. (1977). Analysis of variations in ocean color. *Limonology And Oceanography*, *22*(4), 709–722. http://doi.org/10.4319/lo.1977.22.4.0709
Nechad, B., Ruddick, K. G., & Park, Y. (2010). Calibration and validation of a generic multisensor algorithm for mapping of total suspended matter in turbid waters. *Remote Sensing of Environment*, *114*(4), 854–866. http://doi.org/10.1016/j.rse.2009.11.022
Nurnberg, G. K., & Shaw, M. (1998). Productivity of clear and humic lakes: Nutrients, phytoplankton, bacteria. *Hydrobiologia*, *382*, 97–112. http://doi.org/10.1023/A:1003445406964
Pope, R. M., & Fry, E. S. (1997). Absorption spectrum (380-700 nm) of pure water. II. Integrating cavity measurements. *Applied Optics*, *36*(33), 8710–8723. Retrieved from http://www.opticsinfobase.org/abstract.cfm?&id=63107
Ruddick, K. G., De Cauwer, V., Park, Y.-J., & Moore, G. (2006). Seaborne measurements of near infrared water-leaving reflectance: The similarity spectrum for turbid waters. *Limnology and Oceanography*, *51*(2), 1167–1179. http://doi.org/10.4319/lo.2006.51.2.1167
Scheffer, M. (1998). *Ecology of shallow lakes*. (M. B. Usher, Ed.)*booksgooglecom* (Vol. 1). Chapman & Hall. Retrieved from http://books.google.com/books?hl=en&lr=&id=AVeUo9XHmCMC&oi=fnd&pg=PR9&dq=Ecology+of+Shallow+Lakes&ots=CNjs45VhZF&sig=eNszBfOMNvbQyo2SALKv_ERiiEA
Stephens, S., de Winton, M., Sukias, J., Ovenden, R., Taumoepeau, A., & Cooke, J. (2004). *Rehabilitation of Lake Waikare : Experimental Investigations of the Potential Benefits of Water Level Drawdown*.
Tyler, A. N., Svab, E., Preston, T., Présing, M., & Kovács, W. A. (2006). Remote sensing of the water quality of shallow lakes: A mixture modelling approach to quantifying phytoplankton in water characterized by high-suspended sediment. *International Journal of Remote Sensing*, *27*(8), 1521–1537. http://doi.org/10.1080/01431160500419311
Vant, W. N. (1987). . *Lake Whangape – muddy waters and macrophytes*. Soil and Water (DSIR, Water Quality Centre. Hamilton).
Vidot, J., & Santer, R. (2005). Atmospheric correction for inland waters—application to SeaWiFS. *International Journal of Remote Sensing*, *26*(17), 3663–3682. http://doi.org/10.1080/01431160500034029
Wells, R. D. S.; Vant, W. N.; Clayton, J. F. (1988). Inorganic suspensoids and submerged macrophytes in Lake Whangape, New Zealand. *Verhandlungen, Internationale Vereinigung Für Theoretische Und Angewandte Limnologie*, *23*, 1969–1972.
Westland, S., & Ripamonti, C. (2004). *Computational Colour Science Using MATLAB*. http://doi.org/10.1002/0470020326
Wetzel, R. G. (2001). *Limnology: Lake and River Ecosystems*. *Journal of Phycology* (Vol. 37). Academic Press. http://doi.org/10.1046/j.1529-8817.2001.37602.x

Appendix

Appendix 1. Chromaticity calculations.

Retrieved from:

https://www.semrock.com/how-to-calculate-luminosity-dominant-wavelength-and-excitation-purity.aspx

Reference White (Illuminant)	*x* coordinate	*y* coordinate
CIE-E	0.3333	0.3333
CIE-A	0.4476	0.4075
CIE-C	0.3100	0.3162
CIE-D65	0.3127	0.3291

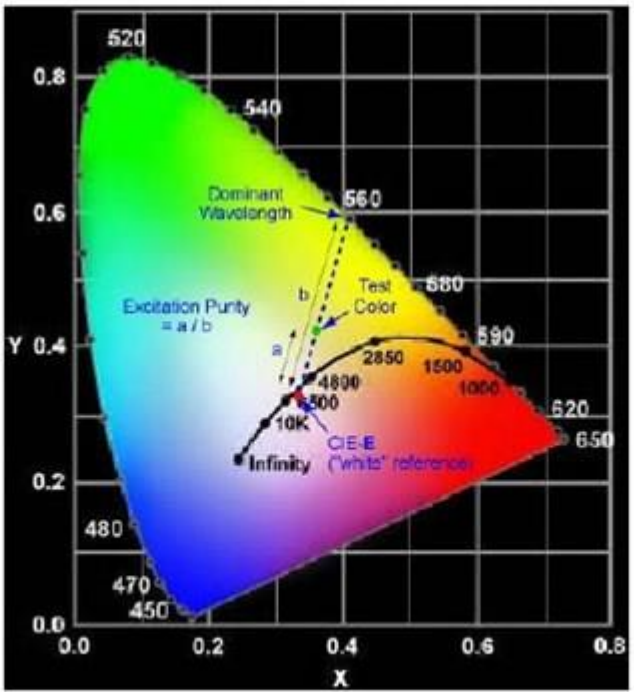

Appendix Table 1. Time series averaged TSS statistics for FWENZ lakes, in order of increasing centroid versus whole lake difference in mean TSS.

FWENZ_ID	Lake name	Mean	Min	Max	Skew	Stddev	n (pixels)	Max of max	Centroid average TSS	Centroid whole lake mean absolute difference
54734	Lake Taupo (Taupomoana)	1.55	-0.66	116.65	15.60	2.05	581676.36	334.05	1.51	0.05
13736		2.62	1.23	5.19	0.32	1.86	4.00	12.33	4.48	1.86
21367	Lake Rotoaira	3.51	0.33	90.73	10.86	3.81	13820.53	330.79	2.59	0.92
21370	Lake Rotopounamu	5.36	0.65	57.66	5.46	6.04	716.18	187.40	3.24	2.12
21383	Lake Otamangakau	5.80	0.51	60.09	3.95	6.33	1036.71	136.44	8.09	2.29
13873	Lake Whakamaru	5.90	0.13	75.27	4.90	6.16	3673.98	171.57	4.31	1.59
13970	Lake Ohakuri	6.28	-0.07	126.53	5.72	8.49	5762.59	478.61	2.48	3.79
13857	Lake Waipapa	6.81	1.03	47.18	3.56	5.72	619.36	133.53	5.50	1.31
13278	Lake Rotongaio	7.02	2.26	50.75	4.89	5.66	262.40	124.43	4.53	2.49
14546	Lake Arapuni	7.29	0.91	75.88	5.13	5.65	5762.67	209.02	4.96	2.33
13876	Lake Maraetai	7.55	1.59	54.83	4.50	5.61	1855.14	122.97	2.91	4.64
14422	Lake Maratoto	8.00	2.70	34.96	2.90	5.17	109.76	85.49	5.30	2.70
13764		8.11	2.48	31.70	1.67	7.58	12.45	97.24	5.26	2.85
13276		8.11	1.93	42.52	2.53	8.65	39.32	98.16	19.46	11.35
14334		8.31	5.20	12.08	0.17	2.88	4.85	55.40	12.32	4.01
13877	Lake Maraetai	8.44	1.68	35.60	2.33	7.12	52.75	131.89	5.59	2.84
12873	Lake Numiti	8.71	4.25	26.84	2.37	3.64	106.00	121.63	7.13	1.58
15061		8.84	5.42	16.08	1.07	2.85	15.63	41.89	12.69	3.85
13687		8.91	6.51	12.07	0.23	2.88	3.00	17.95	10.09	1.18
51371	Upper Mangatawhiri Reservoir	8.95	2.14	66.15	4.42	6.65	615.23	193.63	6.40	2.55
14631		9.40	5.50	14.05	0.40	4.18	3.78	49.15	14.51	5.11
13148	Lake Kuratau	9.70	2.12	95.32	4.70	9.77	700.86	178.56	7.04	2.66
14450		9.81	8.18	11.59	0.05	1.77	2.50	18.62	14.39	4.58
13957	Lake Atiamuri	9.93	1.04	71.18	3.05	8.23	771.03	549.87	7.52	2.41
12830	Lake Harihari	10.15	2.88	41.33	2.50	6.78	84.85	130.43	10.84	0.69
49291	Lake Otamatearoa	10.25	4.94	20.17	0.72	4.17	24.12	66.89	9.87	0.38
12831		10.32	6.69	15.95	0.44	3.34	7.38	47.28	10.98	0.66
14680	Lake Karapiro	10.49	0.95	90.75	3.81	8.31	3207.18	216.77	8.56	1.93
12872	Lake Rotoroa	10.54	4.04	52.89	3.79	6.61	160.15	113.01	7.93	2.61
41472		10.84	5.22	21.17	0.78	5.88	6.75	58.78	11.97	1.13
14428	Lake Rotomanuka	11.20	5.54	32.34	2.61	4.44	91.70	108.48	8.58	2.62
13909	Lake Aratiatia	11.20	1.75	64.44	2.63	9.84	199.17	191.30	10.06	1.14
14179	Lake Ngapouri	11.63	5.20	44.09	3.16	6.04	149.68	107.28	8.11	3.52
51368	Mangatangi Reservoir	11.81	3.17	66.62	3.34	7.58	621.87	211.43	17.72	5.91
14426	Lake Serpentine N	11.82	6.24	26.28	1.58	4.95	24.12	64.92	9.55	2.26
14208	Lake Ngahewa	12.02	6.21	27.67	1.51	4.40	48.86	98.52	10.07	1.95
41470		12.24	6.77	23.60	1.10	4.14	25.58	74.43	10.83	1.40
15022	Lake Rotoroa	12.56	5.86	58.69	4.12	5.99	291.67	160.94	9.71	2.84
13277	Lake Hinemaiaia	12.80	2.27	84.17	3.42	14.85	86.44	268.61	94.10	81.30
14424		13.30	8.60	17.68	0.61	5.13	2.79	64.63	31.35	18.05

51440		13.37	7.97	19.57	0.01	5.19	4.83	35.01	14.68	1.31
12876	Lake Taharoa	13.63	3.91	69.97	3.96	6.76	1649.59	339.77	12.14	1.50
49295	Lake Puketi	14.62	6.04	41.27	2.13	8.66	29.44	93.75	12.86	1.75
14205		15.79	7.59	29.04	0.56	7.45	9.67	122.94	15.10	0.69
12591	Lake Parangi	16.37	8.19	44.53	2.07	7.25	53.85	163.38	16.73	0.36
14071		16.50	9.60	31.26	0.98	6.96	9.83	118.34	18.03	1.53
14427		16.64	9.65	34.68	1.64	5.69	28.49	72.90	17.17	0.53
14720	Lake te ku utu	16.79	7.86	44.34	1.47	9.78	20.41	106.20	17.54	0.75
15008	Lake Cameron	16.81	7.64	40.44	1.41	8.90	17.79	96.94	17.82	1.00
14408	Lake Ruatuna	17.63	10.06	42.53	2.03	6.47	78.35	87.38	14.44	3.19
14405	Lake Mangakaware	17.79	9.22	50.16	2.25	7.83	73.77	129.44	15.27	2.52
14541	Lake Rotongata	17.84	8.51	40.15	1.35	8.23	22.08	113.84	16.49	1.35
49176	Lake Okowhao	18.14	9.59	50.52	2.36	7.96	45.14	188.24	19.02	0.89
15005	Lake Pataka	18.23	10.44	42.40	1.94	8.00	21.80	99.74	19.87	1.64
49194		18.44	11.94	30.51	0.81	6.01	10.17	62.67	20.57	2.12
15035		18.60	10.46	42.93	1.39	9.17	13.79	101.15	18.27	0.33
14802		18.85	13.45	26.43	0.65	6.68	2.44	58.68	30.30	11.44
14772		19.04	13.08	24.97	-0.03	6.22	3.00	109.98	26.79	7.75
14420		19.10	10.96	30.78	0.42	7.02	8.28	80.54	19.55	0.45
15004		19.18	11.25	33.14	0.56	9.15	4.87	74.54	28.03	8.85
15034	Lake Areare	19.19	10.00	59.33	3.00	7.09	222.27	214.41	13.16	6.04
15013	Lake Rotokauri	19.33	10.70	65.15	3.65	7.01	220.67	140.20	14.97	4.36
11084	Lake Orotu	19.50	7.04	43.72	0.63	11.62	12.81	108.07	13.66	5.84
13837		20.08	12.39	28.10	2.25	9.05	2.00	58.93	27.01	6.94
15020		20.30	10.69	41.91	1.45	9.78	10.88	99.64	22.98	2.68
14586	Lake Moananui	20.56	9.16	48.75	1.45	11.60	16.24	132.32	20.40	0.16
21384		20.59	12.82	37.54	0.71	7.93	9.65	105.50	22.35	1.76
15341		20.67	15.32	25.16	-0.15	4.97	3.33	29.59	26.58	5.91
14464		20.97	10.34	46.71	1.14	10.95	13.72	119.10	17.33	3.65
50466		21.07	11.06	36.76	0.46	10.39	6.01	79.96	21.69	0.62
14866		21.49	13.90	30.98	1.87	9.37	2.32	65.14	29.13	7.65
14436		21.78	13.49	29.63	1.30	8.31	3.38	104.37	33.20	11.42
14793		21.95	13.19	33.45	0.55	9.50	3.56	90.54	28.22	6.27
13882		22.31	14.40	30.67	1.12	8.47	2.77	132.52	27.66	5.35
15037	Lake D	22.41	11.87	77.08	3.38	9.19	176.90	596.67	15.64	6.77
20846	Lower Tama	22.44	2.96	297.36	3.11	46.75	129.51	8647.05	8.69	13.75
15033	Lake Hotoananga	22.75	12.41	69.23	2.39	10.25	100.02	170.45	17.08	5.67
14425	Lake Serpentine W	22.90	14.78	33.29	0.25	7.25	5.95	70.05	22.20	0.70
51430		22.95	9.54	57.51	1.19	13.12	20.74	118.28	17.98	4.97
41471		23.16	10.27	56.54	1.14	15.11	9.11	189.40	17.68	5.48
51413		23.28	19.51	28.80	0.98	4.78	2.00	54.24	31.18	7.90
50464		23.67	14.73	51.83	1.66	9.26	24.08	150.10	21.54	2.13
49089		24.19	15.28	32.91	-0.08	6.45	14.00	32.91	35.45	11.26
14718		24.77	11.41	55.04	1.21	12.04	18.66	129.80	38.71	13.94
999008	Port Waikato	25.01	3.90	749.68	7.90	33.86	8227.61	2543.21	14.75	10.26
14657		25.48	22.31	27.49	-0.35	2.78	3.00	27.49	52.59	27.11

15163		25.49	16.12	38.44	0.32	10.49	3.91	84.71	29.34	3.85
15257		25.60	20.00	30.69	0.90	5.89	2.78	72.65	28.47	2.87
12592		25.80	17.68	37.40	0.85	10.97	2.62	99.73	29.77	3.97
49152		25.84	15.85	32.29	-0.51	7.05	4.00	32.29	28.17	2.33
12585		25.86	16.22	35.33	1.02	9.40	3.23	73.68	23.86	2.00
15038	Lake B	26.48	17.66	49.45	1.66	6.25	59.42	133.99	24.75	1.73
49254		26.69	13.79	47.02	0.33	12.42	6.00	94.09	46.27	19.58
14418	Lake Mangahia	26.94	18.84	49.80	1.75	6.52	42.95	108.63	23.39	3.56
15032	Lake Pikopiko	27.04	16.88	54.89	1.64	9.22	25.04	117.98	26.17	0.87
13904		27.76	14.68	42.78	0.09	11.34	5.54	103.28	35.08	7.32
14888		28.07	14.42	43.34	1.55	12.23	5.22	103.54	27.80	0.27
41327		28.33	15.07	43.13	5.49	13.93	2.00	92.80	32.97	4.64
15009		28.69	19.78	40.21	0.79	9.52	3.68	70.36	49.27	20.58
14343		28.80	14.50	53.05	0.49	14.61	6.82	188.70	28.30	0.50
14204		29.32	21.69	36.50	4.04	7.35	2.00	60.50	32.17	2.85
41335		29.80	15.31	43.13	0.26	15.06	2.76	88.92	45.78	15.98
49090	Lake Ohinewai	29.82	18.11	85.44	3.00	10.57	114.09	197.57	23.44	6.38
15176		29.98	14.62	72.64	1.31	15.51	25.40	131.29	21.94	8.04
51282		30.09	22.27	39.02	0.92	9.15	3.00	151.17	35.84	5.76
49091	Lake Rotokawau	30.52	19.93	60.61	2.20	7.04	86.18	298.56	28.65	1.87
15165		30.82	25.65	33.38	3.32	4.44	2.17	43.83	46.35	15.53
8266		32.17	21.02	44.02	1.08	10.76	3.70	151.63	37.85	5.68
51404		32.53	21.89	44.97	1.00	12.42	2.68	122.61	31.14	1.39
20851	Upper Tama	32.59	2.18	515.55	3.70	71.96	201.63	19343.60	8.42	24.17
13950		33.06	18.03	62.15	0.83	13.53	12.28	169.96	29.53	3.53
14121		33.37	22.10	49.43	0.81	11.10	5.30	182.21	36.55	3.18
14406	Lake Ngaroto	34.21	19.14	94.11	2.56	9.59	701.19	340.36	26.23	7.98
14559		35.10	28.99	41.91	0.32	7.33	2.73	313.99	41.55	6.45
999019	Whitianga Harbour	35.35	2.61	317.45	3.27	38.81	5263.04	619.93	32.27	3.07
999011	Tairua Harbour	35.63	4.63	244.07	2.36	32.28	2735.27	618.62	17.06	18.57
49148		35.96	23.26	55.57	0.35	12.87	5.89	144.37	40.05	4.09
15106		36.58	24.35	49.17	-0.08	11.16	3.67	64.93	43.29	6.72
50783		36.96	21.20	53.35	0.61	21.90	2.00	88.17	42.92	5.96
14723		37.74	26.32	50.48	0.74	12.12	3.40	159.23	44.57	6.83
14860	Hamareha Lakes	38.14	28.44	43.14	4.10	9.40	4.67	115.67	25.57	12.58
15122		38.23	29.33	51.53	0.52	7.07	11.74	142.57	40.41	2.19
12588		38.52	29.69	49.47	0.85	10.38	3.07	128.35	45.25	6.72
50768		38.92	25.67	52.18	0.00	18.74	2.00	52.18	52.18	13.26
13284		38.96	27.39	54.41	0.82	9.26	11.29	155.21	39.61	0.65
14407		40.06	28.09	60.78	0.70	10.56	10.13	117.61	38.20	1.86
49189		40.96	30.17	53.26	0.46	10.56	4.92	97.45	41.45	0.50
15036		41.55	32.33	58.34	0.89	8.46	8.27	209.54	47.52	5.97
999002	Kennedy Bay	41.58	8.29	148.21	1.27	31.64	76.55	296.72	24.61	16.97
15007	Lake Koromatua	41.98	33.84	54.00	0.53	4.94	25.29	186.07	40.62	1.36
49186	Lake Rotongaro	42.57	19.40	145.87	3.04	13.61	2139.64	879.91	38.24	4.33
50470	Lake Kopuera	44.25	28.03	95.71	2.27	10.06	318.40	371.91	32.98	11.27

49200	Lake Hakanoa	45.09	26.56	103.01	2.35	9.47	419.60	193.41	37.56	7.53
14542		45.21	31.97	59.11	3.77	14.06	2.42	168.56	47.94	2.73
41328		45.43	33.58	59.67	1.17	12.81	3.59	134.09	44.66	0.77
14562		45.74	34.07	57.42	0.00	16.51	2.00	79.30	41.07	4.68
50781		45.75	35.55	61.71	0.41	10.85	5.30	189.25	53.42	7.67
999007	Pakoka Stream	46.14	34.54	68.75	1.52	14.92	2.67	93.59	39.54	6.60
15270		46.23	36.84	59.17	7.40	6.88	2.00	59.17	41.43	4.81
14146		46.57	34.47	67.37	1.47	15.24	2.54	499.35	68.29	21.73
51380		48.19	28.37	108.26	1.79	18.85	38.57	431.99	65.84	17.65
49156		49.06	34.54	78.22	0.91	13.02	15.23	197.07	52.69	3.64
49257		49.26	44.65	#DIV/0!	6.52	2.00		0.00	98.47	49.21
49181		49.57	40.28	40.19	7.91	5.39	2.25	77.13	144.43	94.86
49076		49.72	38.45	64.73	0.32	11.23	4.52	291.19	51.00	1.28
50255		50.38	39.22	61.53	0.00	15.77	2.00	92.56	63.36	12.98
13149		51.53	28.19	87.84	1.40	19.70	8.66	226.32	56.69	5.16
14999		51.59	41.51	59.62	3.44	7.32	3.25	128.75	63.55	11.96
15170		53.15	41.07	65.23	0.00	17.08	2.00	109.41	37.55	15.61
14082	Lake Ngakoro	54.24	25.51	92.46	0.49	15.86	34.14	207.37	62.33	8.09
999009	Purangi River	54.41	13.29	213.82	1.71	36.27	306.70	521.06	47.50	6.91
49169		55.80	35.99	127.11	2.21	16.13	108.70	271.73	46.08	9.72
999006	Otahu River	59.37	21.59	177.90	1.73	30.25	192.99	378.68	66.15	6.77
21356		60.05	37.46	99.52	2.53	18.63	10.16	188.33	54.02	6.03
999018	Wharekawa Harbour	61.22	12.12	294.57	1.85	51.86	432.69	708.29	31.47	29.75
13147		61.31	54.34	68.15	-0.02	5.65	4.00	68.15	61.25	0.06
999001	Colville Bay	63.32	18.50	189.19	1.99	23.03	628.25	375.66	20.84	42.49
50254		63.34	34.09	124.18	0.82	28.39	12.01	319.05	57.60	5.75
14157		64.36	42.14	101.42	0.48	23.62	5.82	287.53	48.37	15.99
999003	Manaia Harbour	64.40	10.07	366.00	2.38	56.35	1360.11	1133.41	30.20	34.20
999017	Whangapoua Harbour	64.87	3.39	456.39	2.42	70.78	5405.64	977.15	9.36	55.50
999016	Whangamata Harbour	64.99	8.09	267.41	2.26	48.89	1918.83	619.63	45.39	19.60
49180	Lake Whangape	66.67	19.60	216.76	1.71	21.86	7251.50	507.46	51.60	15.06
13886		70.86	60.28	89.49	0.99	11.05	4.08	432.60	44.75	26.11
999015	Waiau River	71.54	15.57	282.68	1.98	39.49	1122.06	751.61	62.95	8.59
41314	Lake Waahi	73.33	33.77	208.53	2.41	16.75	3417.33	431.70	62.08	11.25
49187	Lake Rotongaroiti	75.69	46.99	151.65	1.52	17.84	295.67	1156.49	65.77	9.92
13915	Lake Rotokawa	76.43	30.86	183.78	1.09	27.89	504.33	605.33	71.54	4.90
49258		77.69	61.09	99.36	0.05	19.35	3.50	161.57	64.81	12.89
50782	Lake Waikare	119.70	28.86	306.47	1.31	32.95	25845.21	1151.46	111.26	8.44
49199		119.85	102.37	143.71	0.36	14.73	7.52	317.37	120.78	0.93
49228		125.72	114.85	129.82	0.59	11.27	3.52	847.30	117.08	8.64
13883		140.19	82.43	213.24	6.77	54.42	6.38	647.72	205.92	65.72
49238		180.80	154.94	208.11	0.23	20.80	6.13	1478.67	193.66	12.86
49239	Lake Kimihia	315.05	185.67	430.45	0.08	47.56	287.89	1430.16	299.74	15.32
999013		388.47	191.88	602.57	67.70	172.28	2.70	2102.55	43.53	344.94
20857	Blue Lake	2627.63	1960.89	3583.86	2.43	494.67	96.90	36456.70	2296.73	330.90
20852		4325.30	4032.92	4629.17	-0.08	302.11	2.75	15865.70	8090.73	3765.42

20853		12544.86	10899.69	13882.61	5.44	660.47	10.10	38755.00	17998.06	5453.20
54734	Lake Taupo (Taupomoana)	1.55	-0.66	116.65	15.60	2.05	581676.36	334.05	1.51	0.05
13736		2.62	1.23	5.19	0.32	1.86	4.00	12.33	4.48	1.86
21367	Lake Rotoaira	3.51	0.33	90.73	10.86	3.81	13820.53	330.79	2.59	0.92

Appendix Table 2. All FWENZ lakes displayed in the order of increasing average dominant wavelength, alongside average values of purity, chromaticity coordinates and TSS (mg L^{-1}). An approximate indicative wavelength colour ramp has been applied to visualise dominant wavelength.

FWENZ ID	FWENZ name	Geomorphic	Purity	Dominant wavelength	x	y	z	TSS
20852		Volcanic	0.30	483.84	0.33	0.33	0.35	1500.75
14430		Riverine	0.31	493.44	0.27	0.34	0.39	18.20
14820		Riverine	0.32	494.00	0.18	0.36	0.46	9.63
54734	Lake Taupo (Taupomoana)	Volcanic	0.32	494.49	0.13	0.36	0.52	1.56
20851	Upper Tama	Volcanic	0.32	494.54	0.18	0.37	0.45	8.08
14860	Hamareha Lakes	Riverine	0.32	494.91	0.29	0.34	0.37	54.34
15341		Riverine	0.32	495.02	0.24	0.36	0.40	24.18
14436		Peat	0.33	495.28	0.26	0.35	0.38	18.28
14718		Dam	0.33	495.61	0.27	0.35	0.38	12.22
20857	Blue Lake	Volcanic	0.35	496.65	0.18	0.39	0.43	1542.62
13904		Riverine	0.35	496.84	0.23	0.37	0.40	20.87
14917		Dam	0.36	497.67	0.29	0.35	0.36	56.18
20858	Beggs Pool	Dam	0.37	498.14	0.27	0.36	0.36	34.61
8266		Shoreline	0.37	498.24	0.25	0.38	0.37	15.51
13883		Riverine	0.38	498.70	0.31	0.35	0.34	10.21
15240		Riverine	0.38	499.55	0.23	0.40	0.38	26.93
15009		Peat	0.38	499.61	0.23	0.39	0.37	29.78
20846	Lower Tama	Volcanic	0.34	499.84	0.22	0.36	0.42	10.14
11096		Riverine	0.40	500.96	0.27	0.38	0.35	33.66
15112		Riverine	0.41	501.32	0.26	0.39	0.35	28.09
15165		Riverine	0.41	501.77	0.25	0.40	0.35	43.68
14573			0.42	502.10	0.21	0.43	0.36	12.73
11084	Lake Orotu	Volcanic	0.42	502.29	0.29	0.36	0.34	21.67
14423	Lake Rotopataka	Peat	0.42	502.38	0.22	0.42	0.36	31.88
14922		Riverine	0.43	503.02	0.24	0.41	0.35	14.96
999012			0.44	503.36	0.27	0.39	0.34	33.01
51404			0.45	504.08	0.27	0.39	0.34	42.66
41327		Riverine	0.45	504.36	0.26	0.39	0.34	39.47
51440		Dam	0.32	504.38	0.27	0.35	0.38	14.14
14902		Riverine	0.46	504.54	0.21	0.46	0.34	36.63
49258		Riverine	0.46	504.64	0.23	0.44	0.34	21.52
21370	Lake Rotopounamu	Volcanic	0.39	504.77	0.16	0.44	0.40	2.10
14542		Riverine	0.45	505.26	0.28	0.39	0.34	45.28
15025		Riverine	0.47	505.75	0.27	0.40	0.33	55.70
15140		Riverine	0.47	506.02	0.22	0.44	0.34	39.57
14546	Lake Arapuni	Dam	0.39	506.22	0.22	0.40	0.37	4.77
14422	Maratoto	Peat	0.35	506.52	0.25	0.37	0.39	4.83
14802		Riverine	0.48	506.56	0.24	0.43	0.33	31.18
13857	Lake Waipapa	Dam	0.39	506.79	0.22	0.40	0.38	5.12
14157	Lake Whangioterangi (Echo Lake)	Geothermal	0.34	506.82	0.24	0.37	0.39	63.32
14146		Dam	0.49	506.89	0.25	0.42	0.33	60.00
51282		Dam	0.49	507.06	0.25	0.43	0.32	41.35

49254		Riverine	0.44	508.01	0.22	0.44	0.33	24.42
20853		Volcanic	0.31	508.40	0.34	0.34	0.32	21074.93
41472		Dam	0.40	508.58	0.24	0.40	0.36	13.32
13833		Dam	0.49	508.71	0.28	0.39	0.33	79.58
49291	Lake Otamatearoa	Aeolian	0.37	509.08	0.23	0.39	0.37	8.47
49181		Riverine	0.52	509.15	0.28	0.40	0.32	38.01
12831	Lake Rototapu	Aeolian	0.42	509.28	0.28	0.38	0.35	16.75
14424	Lake Serpentine E	Peat	0.52	509.64	0.24	0.45	0.31	36.24
12873	Lake Numiti	Aeolian	0.40	509.76	0.25	0.39	0.35	7.37
14425	Lake Serpentine W	Peat	0.53	509.95	0.26	0.43	0.31	21.33
12872	Lake Rotoroa	Aeolian	0.41	509.99	0.25	0.40	0.35	7.82
13276		Dam	0.38	510.36	0.24	0.38	0.38	7.65
14426	Lake Serpentine N	Peat	0.44	510.38	0.28	0.39	0.34	9.47
50783		Riverine	0.52	510.43	0.26	0.43	0.31	59.27
14678		Riverine	0.53	511.09	0.24	0.46	0.30	57.14
12830	Lake Harihari	Aeolian	0.40	511.44	0.26	0.39	0.35	16.80
21367	Lake Rotoaira	Volcanic	0.35	511.91	0.19	0.40	0.41	2.27
50462		Riverine	0.53	511.99	0.25	0.44	0.30	38.15
15060		Riverine	0.47	512.11	0.26	0.41	0.32	29.60
999017			0.41	512.14	0.21	0.42	0.38	8.33
21383	Lake Otamangakau	Aeolian	0.39	513.03	0.26	0.38	0.36	7.80
49295	Lake Puketi	Aeolian	0.42	513.24	0.26	0.39	0.35	19.30
13970	Lake Ohakuri	Dam	0.35	513.38	0.21	0.40	0.39	2.55
13882		Riverine	0.35	513.73	0.31	0.35	0.34	25.05
49076		Aeolian	0.43	513.81	0.27	0.40	0.32	30.82
14680	Lake Karapiro	Dam	0.43	514.06	0.26	0.40	0.34	9.37
14586	Lake Moananui	Dam	0.47	514.12	0.28	0.40	0.32	22.81
15651		Riverine	0.43	514.38	0.26	0.41	0.33	12.48
12591	Lake Parangi	Aeolian	0.46	514.40	0.25	0.42	0.32	19.91
13278	Lake Rotongaio	Volcanic	0.41	514.57	0.22	0.42	0.35	4.29
51413			0.45	514.58	0.29	0.40	0.32	31.93
13950		Peat	0.43	514.67	0.26	0.40	0.34	28.76
13909	Lake Aratiatia	Dam	0.37	514.79	0.25	0.39	0.36	18.81
999011			0.40	514.84	0.27	0.38	0.35	18.03
13148	Lake Kuratau	Dam	0.37	514.90	0.26	0.38	0.36	6.62
14205	Rotowhero (Green Lake)	Geothermal	0.52	514.93	0.24	0.46	0.29	18.94
51371	Upper Mangatawhiri Reservoir	Dam	0.41	514.97	0.23	0.41	0.36	5.56
21384	Lake Rotokura	Volcanic	0.36	515.43	0.28	0.36	0.36	21.90
13876	Lake Maraetai	Dam	0.37	515.71	0.22	0.40	0.38	2.61
49257		Riverine	0.56	516.19	0.24	0.49	0.27	49.80
51430		Riverine	0.43	516.20	0.25	0.41	0.34	17.84
15022	Lake Rotoroa	Peat	0.45	516.85	0.29	0.38	0.33	9.17
21371	0.00	Volcanic	0.46	516.92	0.29	0.39	0.33	31.90
41471	0.00	Riverine	0.45	517.16	0.25	0.41	0.34	27.62
14428	Lake Rotomanuka	Peat	0.44	517.29	0.29	0.38	0.33	8.75
14208	Lake Ngahewa	Volcanic	0.43	517.44	0.29	0.39	0.32	9.23

15634		Riverine	0.33	517.65	0.31	0.42	0.27	31.33
13957	Lake Atiamuri	Dam	0.38	517.72	0.24	0.40	0.36	7.48
15170		Riverine	0.56	517.80	0.26	0.46	0.28	17.93
12876	Lake Taharoa	Aeolian	0.44	517.82	0.26	0.41	0.33	11.40
51368	Mangatangi Reservoir	Dam	0.46	517.90	0.26	0.41	0.33	23.87
14723		Riverine	0.48	518.13	0.27	0.41	0.31	39.61
15061		Riverine	0.42	518.35	0.27	0.39	0.34	13.74
13877	Lake Maraetai	Dam	0.36	518.72	0.24	0.39	0.38	5.37
14631		Peat	0.42	518.78	0.29	0.38	0.33	20.45
41335		Riverine	0.46	519.01	0.30	0.39	0.31	37.35
13873	Lake Whakamaru	Dam	0.36	519.21	0.24	0.39	0.37	3.98
15008	Lake Cameron	Peat	0.46	520.34	0.27	0.40	0.33	24.59
41470		Riverine	0.41	521.15	0.25	0.40	0.35	11.48
14720	Lake te ku utu	Riverine	0.46	522.10	0.29	0.39	0.32	17.07
12588		Aeolian	0.48	523.09	0.29	0.41	0.30	46.04
50469		Dam	0.46	523.11	0.29	0.40	0.31	33.22
13837		Riverine	0.46	523.18	0.29	0.42	0.29	39.53
14888	Lake Okoroire	Peat	0.55	523.32	0.29	0.42	0.29	75.44
13907		Riverine	0.41	523.33	0.29	0.38	0.33	54.89
14071	Lake Tutaeinanga	Volcanic	0.49	523.74	0.29	0.41	0.29	26.21
51383		Dam	0.51	524.20	0.30	0.41	0.29	61.66
999019			0.42	524.39	0.28	0.39	0.32	25.77
14082		Volcanic	0.53	524.42	0.28	0.43	0.29	94.28
14464		Peat	0.45	525.06	0.29	0.41	0.30	20.89
999003			0.43	525.24	0.26	0.40	0.33	27.03
14408	Lake Ruatuna	Peat	0.43	525.35	0.30	0.38	0.31	13.33
12592		Aeolian	0.48	525.61	0.31	0.38	0.31	53.25
14343		Dam	0.48	525.76	0.30	0.41	0.29	49.81
13915	Lake Rotokawa	Geothermal	0.53	526.18	0.28	0.44	0.28	92.15
14541	Lake Rotongata	Peat	0.45	526.19	0.30	0.39	0.31	27.68
14420		Peat	0.47	526.46	0.30	0.41	0.29	37.89
49151		Riverine	0.42	526.65	0.31	0.41	0.28	59.66
999018			0.43	526.71	0.27	0.40	0.33	29.48
49147		Riverine	0.47	527.47	0.29	0.40	0.31	44.75
34200		Volcanic	0.47	527.51	0.29	0.41	0.30	22.24
15033	Lake Hotoananga	Peat	0.44	527.75	0.29	0.40	0.30	17.27
999009			0.43	528.87	0.28	0.39	0.33	41.43
14179	Lake Ngapouri	Volcanic	0.47	529.74	0.29	0.41	0.30	8.07
14587		Riverine	0.45	530.14	0.33	0.41	0.25	40.60
51380		Dam	0.50	530.37	0.32	0.37	0.31	140.11
15035	Lake A	Peat	0.44	530.71	0.31	0.38	0.31	24.93
14885		Peat	0.50	530.82	0.29	0.44	0.27	50.69
14405	Lake Mangakaware	Riverine	0.45	531.26	0.31	0.39	0.30	14.11
15176		Riverine	0.47	531.69	0.30	0.40	0.29	22.95
15037	Lake D	Peat	0.42	533.17	0.31	0.38	0.31	16.42
50781		Peat	0.45	533.44	0.32	0.38	0.30	43.85

999016			0.41	533.85	0.29	0.39	0.32	36.68
12585		Aeolian	0.47	534.18	0.31	0.40	0.29	25.64
999015			0.40	534.23	0.29	0.39	0.32	54.60
51406			0.36	534.95	0.33	0.40	0.27	29.35
14334		Riverine	0.44	535.25	0.31	0.39	0.29	20.91
49176	Lake Okowhao	Riverine	0.41	535.39	0.32	0.37	0.31	24.10
49148		Riverine	0.46	535.84	0.31	0.42	0.28	86.62
15039	Lake C	Peat	0.39	536.28	0.32	0.38	0.30	31.43
14866		Riverine	0.45	536.32	0.34	0.38	0.28	23.25
999006			0.44	536.73	0.31	0.38	0.31	58.21
999008			0.41	536.88	0.31	0.39	0.29	14.53
15032	Lake Pikopiko	Peat	0.43	537.34	0.32	0.39	0.29	30.44
15396	0.00	Riverine	0.42	537.48	0.31	0.48	0.21	34.55
14427	0.00	Peat	0.42	541.70	0.32	0.38	0.30	17.85
14772	0.00	Riverine	0.40	541.77	0.32	0.41	0.27	56.38
15005	Lake Pataka	Peat	0.42	541.90	0.33	0.38	0.30	23.63
15013	Lake Rotokauri	Peat	0.43	545.92	0.33	0.38	0.29	14.15
15122		Riverine	0.38	546.49	0.33	0.40	0.28	42.97
15036	Lake E	Peat	0.35	546.77	0.32	0.40	0.28	64.72
14559		Riverine	0.39	548.35	0.33	0.40	0.27	43.49
15106		Riverine	0.36	549.87	0.32	0.50	0.18	16.57
49194		Riverine	0.38	550.71	0.34	0.37	0.29	30.39
49091	Lake Rotokawau	Peat	0.36	551.55	0.34	0.37	0.29	27.68
50464		Peat	0.34	553.97	0.34	0.36	0.30	22.54
50254		Riverine	0.39	554.37	0.34	0.39	0.27	69.09
49180	Lake Whangape	Riverine	0.32	554.79	0.34	0.40	0.26	51.27
15020	Horseshoe Lake	Peat	0.44	555.38	0.32	0.39	0.29	31.95
49200	Lake Hakanoa	Riverine	0.33	555.52	0.34	0.40	0.26	37.95
50466		Peat	0.34	556.94	0.33	0.35	0.32	21.81
14406	Lake Ngaroto	Peat	0.31	560.78	0.34	0.39	0.27	27.35
14407	Lake Ngarotoiti	Peat	0.30	561.04	0.35	0.38	0.27	54.39
14998		Riverine	0.30	561.47	0.35	0.39	0.26	78.75
41314	Lake Waahi	Riverine	0.35	562.31	0.35	0.39	0.26	62.08
15038	Lake B	Peat	0.33	562.42	0.35	0.36	0.29	24.51
49186	Lake Rotongaro	Riverine	0.32	564.00	0.35	0.38	0.27	38.78
13149		Dam	0.29	564.40	0.35	0.37	0.28	55.14
15034	Lake Areare	Peat	0.35	564.57	0.35	0.35	0.30	13.26
50782	Lake Waikare	Riverine	0.29	566.19	0.36	0.40	0.24	122.43
50470	Lake Kopuera	Riverine	0.31	566.38	0.36	0.38	0.26	32.93
15007	Lake Koromatua	Peat	0.30	566.50	0.36	0.38	0.26	42.26
49156		Riverine	0.34	568.67	0.36	0.38	0.27	63.82
49238		Riverine	0.45	570.49	0.39	0.34	0.27	29.30
49090	Lake Ohinewai	Riverine	0.34	571.58	0.36	0.36	0.29	23.65
49187	Lake Rotongaroiti	Riverine	0.27	572.65	0.37	0.39	0.24	71.13
13284	Pukuriri Lagoon	Volcanic	0.32	574.53	0.36	0.38	0.25	33.51
15029		Riverine	0.24	574.59	0.43	0.46	0.10	10.70

14418	Lake Mangahia	Peat	0.32	575.66	0.36	0.35	0.28	23.07
49169		Riverine	0.29	575.72	0.37	0.37	0.26	46.43
49199		Riverine	0.26	579.35	0.39	0.38	0.24	121.37
49259		Riverine	0.24	580.09	0.37	0.37	0.26	243.88
49239	Lake Kimihia	Riverine	0.25	581.42	0.38	0.38	0.24	283.41
49228		Riverine	0.31	597.71	0.38	0.34	0.28	99.23
49189		Riverine	0.46	610.00	0.41	0.35	0.24	32.97
13764		Riverine	0.33	613.47	0.42	0.33	0.25	2.28
49196	Lake Waiwhata	Riverine	0.36	618.80	0.46	0.33	0.21	3.62
49089		Riverine	0.36	621.21	0.50	0.32	0.18	4.75
999001			0.37	625.25	0.39	0.33	0.28	46.22
14999		Riverine	0.33	647.10	0.45	0.34	0.21	117.74
13736	Lake Rotokotuku	Riverine	0.39	651.79	0.49	0.31	0.20	3.51
15141		Riverine	0.42	715.32	0.49	0.30	0.21	4.95